M. Minty
12/22/98

HIGHLIGHTS (12/7-12/18):

commissioning of 5th extraction line wire (Hayano)
new extraction line optics which give good phase space coverage in both x and y at wire scanners (Kubo) and not too small beam sizes at wires
damping ring vertical dispersion correction to less than ~~2 cm~~ ±2 cm peak-to-peak (Kubo/Urakawa)
injector studies (front end phasing for 20 ps bunch length and minimum energy spread) (JLT/Hayano/Vogel/Minty) — < 5% FULL-WIDTH
detailed 4-D beam matrix reconstruction using 5-wire extraction line emittance measurements:

MEASURED	\eps_x,p = (1.73 +/- 0.14)e-9 m-r
	\eps_y,p = (4.11 +/- 0.16)e-11 m-r
INTRINSIC	\eps_x,i = (1.73 +/- 0.14)e-9 m-r
	\eps_y,i = (1.40 +/- 0.16)e-11 m-r

(consistent with 0.8% coupling)
(MDW/JLT/Minty)
extraction line double-kicker versus single kicker orbit rms measurements (Okugi)

LOWLIGHTS (12/7-12/18):

BSOIC trip with extraction line bends off causing KEKB beam abort
modulator HV connector troubles (no damping ring beam for SLAC studies until Monday 12/14)
degradation of interferometer optics apparant during week of 12/14-12/18
linac klystron 3 electronic phase shifter drifts producing highly variable beam currents 12/16-12/17
frequent east-hall BSOIC trips (even without beam)

	M	T	W	R	F
WEEK OF 12/7/98	turn on at ~18:00 multiple fringe fit new ELwire commissioning DR ν_y correction BSOIC trip $\epsilon_x^{EL} = 3.4 \times 10^{-9}$ m-r (BUMAG$_x$ = 1.4) $\epsilon_y^{EL} = 7.5 \times 10^{-11}$ m-r $\epsilon_y^{EL} \simeq 5.0 \times 10^{-11}$ m-r (w/ DR bumps) } 12/7-9/98		1.73/3.22/ 1.59/1.67/ 1.07/0.32 (ARRIVE AT MTF) mod #3 trouble @ 23:30	injector studies $\phi_{L\phi} = -6.5°$ $\phi_{SBS} = 27.5°$ for $\sigma_z^{rms} = 20$ps & < 5% FW σ_δ (NO LINAC/DR BEAM)	(NO LINAC/ DR BEAM)
WEEK OF 12/14/98	turn on at ~18:00 new EL optics $\epsilon_x^{EL} = 1.7 \times 10^{-9}$ m-r $\epsilon_y^{EL} = 5.7 \times 10^{-11}$ m-r $\epsilon_y^{EL} = 5.0 \times 10^{-11}$ m-r (w/ EL ν_y correction)	2.4/1.9/1.8/ 0.8/0.6/0.3 injector studies w/ $\delta\phi_{LINAC} = +2/0°$ 2.5/1.8/1.7/ 0.8/0.8/0.8 dual interferometer setup double kicker studies	EL 4-D emittance msrmts. incl'g ν_x, ν_y interferometer studies tune restore to 11/98 beam energy msrmt. vs. time	EL ϵ_y vs. DR σ_y msrmts. incl'g β_y, ν_y tune monitor setup injector current jitter studies magnet restore to 11/98	DR σ_x msrmt. $\epsilon(\gamma)$ tune monitor work $\sigma_{x,y,\Delta s}$ (I) msrmts. bend tweak kicker studies

discussion w/ H²

date	DR coupling	EL coupling
11/98	1.4%	2.4%
11/20/98	0.6%	3.1%
12/7 week	1.1%	3.8%
12/14 week	3.2%	3.8%

← APPARENT PROBLEM

索　　引

摘　　要　　頁 数　　摘　　要　　頁 数　　摘　　要

Covered by 11
from 4/98 K. KUBO

drlbw44 based on new parameters of Bends (a little different from design)

xtune=15.142244　　xphase/cell=132.8 deg
ytune=8.719839　　yphase/cell=45.6 deg

Closed orbit:

	x	px/p0	y	py/p0	z	dp/p0
Entrance :	-1.36E-5	-1.18E-5	.000000	.000000	-1.13E-4	.002001
Exit :	-1.36E-5	-1.18E-5	.000000	.000000	-1.13E-4	.002001

Design momentum P0 = 1.3000000 GeV Revolution freq. f0 = 2163631.9 Hz
Energy loss per turn U0 = .0434936 MV Effective voltage Vc = .2500000 MV
Equilibrium position dz = 11.685409 mm Momentum compact. alpha = .0021261
Orbit dilation dl = -1.987640 mm Effective harmonic # h = 330.00067
Bucket height dV/P0 = .0113778

Imag.tune:	0.0000000	0.0000000	0.0000000
Real tune:	0.1422262	-0.2802441	-0.0045986

$\tau_x = 17.4$ ms
$\tau_y = 27.7$ ms
$\tau_\epsilon = 19.5$ ms

Damping per one revolution:
X : -2.642624E-05　Y : -1.669492E-05　Z : -2.365803E-05
Damping time (sec):
X : 1.748965E-02　Y : 2.768422E-02　Z : 1.953611E-02
Tune shift due to radiation:
X : -5.921195E-08　Y : -4.385649E-09　Z : 1.741234E-10
Damping partition number:
X : 1.5829　Y : 1.0000　Z : 1.4171

Emittance X = 1.08030E-9 m　Emittance Y = .00000000 m
Emittance Z = 3.07155E-6 m　Energy spread = 5.48906E-4
Bunch Length = 5.59592779 mm　Beam tilt = .00000000 rad
Beam size xi = .10354823 mm　Beam size eta = .00000000 mm

Parameters with intrabeam scattering:
Particles/bunch = 1.00000E10　Minimum coupling = 1.00000000 %
Emittance X = 1.50520E-9 m　Emittance Y = 1.5053E-11 m
Emittance Z = 5.05561E-6 m　Energy spread = 7.04215E-4
Bunch Length = 7.17926056 mm　Beam tilt = .00000000 rad
Beam size xi = .12778864 mm　Beam size eta = 3.18740E-4 mm

$\varepsilon_x = 1.51 \times 10^{-9}$ m.r
$\varepsilon_y = 0.01\,\varepsilon_x = 1.51 \times 10^{-11}$ m.r

Summary of Accelerator Physics Studies at KEK/ATF Dec. 8-Dec. 21, 1998

M. Minty, J. Turner, M. Woodley
SLAC, Stanford University, Stanford, CA, USA
H. Hayano, K. Kubo, V. Vogel
KEK, Ibaraki, Japan
T. Okugi
Tokyo Metro. Univ., Tokyo, Japan

1. Introduction

During our stay at KEK, various studies were undertaken of the injector, damping ring, and extraction line at the ATF. In the injector, we investigated the beam energy spread and bunch length as a function of RF phase and amplitude controls. In the damping ring and extraction line, we concentrated on 4 dimensional beam phase space measurements made using all 5 available wire scanners in the extraction line. The measured intrinsic beam emittance ratio is well within the ATF design goal of 1%.

2. Injector Studies

The injector studies were motivated by the recent ATF Reports of A.D. Yeremian, T. Kotseroglou and V. Vogel. The bunching system consists of two subharmonic bunchers, a 0.75c s-band buncher and the accelerator section L0. Previously the energy spread became large when the bunch length was minimized at the L0 exit. The goal of our study was to change this relationship in order to optimize both of these beam parameters simultaneously.

The beam was transported to an 80 MeV analyzing dump and digitized with a beam profile monitor. The width between cross-hairs of the screen was measured to be about 0.2 amperes on the analyzing spectrometer bend magnet, corresponding to about 0.8% of the total beam energy. Dips in the data due to the cross-hairs can be seen (note figure 1). The magnet was scanned to piece together a single beam profile over some qualitatively representative range. The initial look at the energy profile shown in Figure 1, indicated the situation was not much changed from the >20% energy spread seen previously.

20K MAX

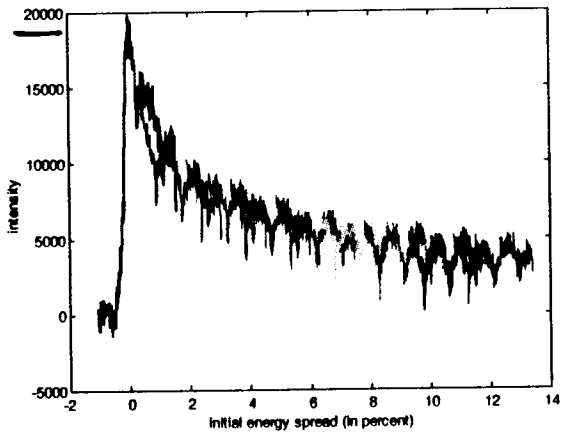

WITIAL ENERGY SPREAD AT 80 MeV

(FULL SCALE 16%)

Figure 1 Digitized profile monitor pictures pieced together showing initial energy spread at 80 MeV.

While monitoring the bunch length and energy spread, scans were then done of the s-band buncher phase versus L0 phase, followed by scans of sub-

harmonic buncher phases and s-band buncher amplitude.

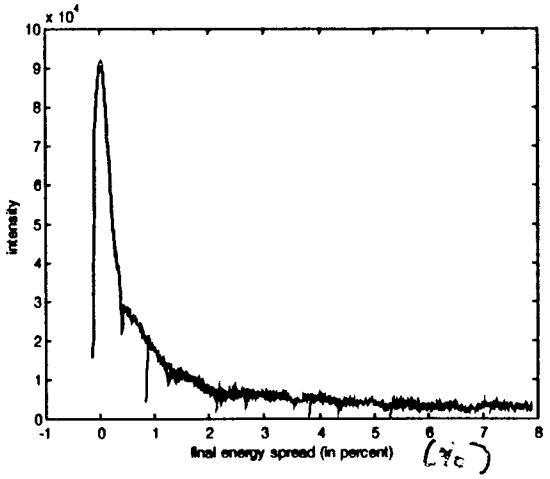

Figure 2 Digitized profile monitor pictures pieced together showing final energy spread at 80 MeV.

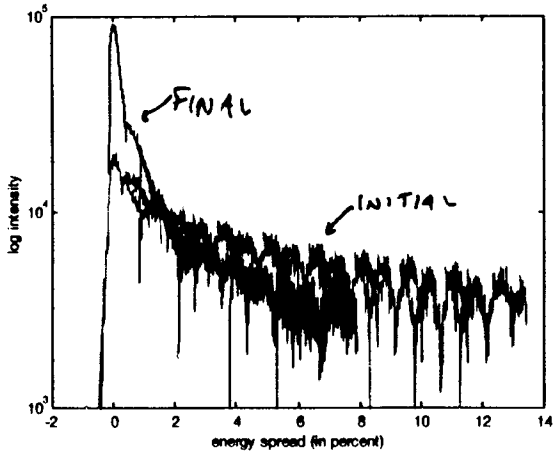

Figure 3 Digitized profile monitor pictures pieced together showing initial (red) and final (green) energy spread at 80 MeV. Intensity on the screen is shown on a log scale to accentuate the difference in the low energy tails.

Figure 2 shows the energy spread after setting these parameters to their optimal values. Figure 3 shows the initial energy profile overlaid with the final energy profile. A log scale is used on the vertical axis to better show the difference in the tails of the distributions. A clear factor of 1.3 increase in the area between 0-5% is evident.

In Figs. 1-3 background has been subtracted. Figure 4 shows the raw signal, without background correction, in the final case. Overlaid are the first and last data sets used to make the composite, and the background. This shows that the low energy tail of the distribution is near the background level.

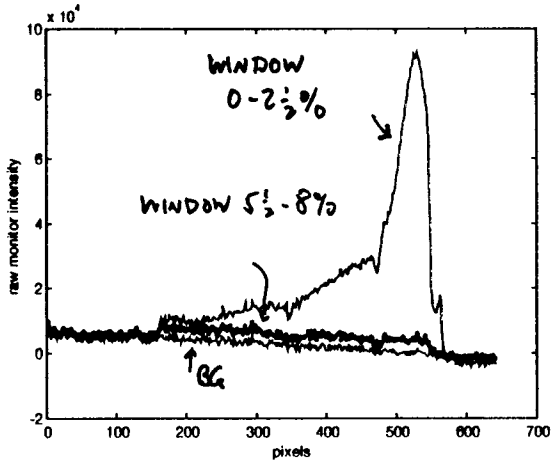

Figure 4 Overlay of raw digitized data with background trace (blue) on bottom. The tall trace (green) on top is the first frame which goes from 0 to about 2 ½%. The middle trace is the last frame which goes from 5 ½ to about 8%.

In contrast, the initial case is given in Fig. 5 which shows the low energy tail higher above background even at 13% rather than the 8% tail shown in Fig. 4.

INITIAL

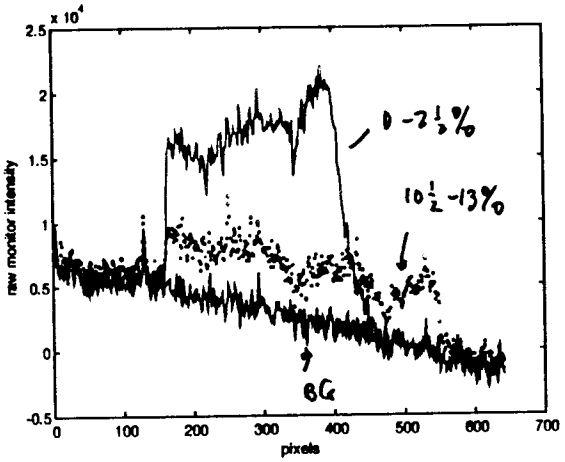

Figure 5 Overlay of raw digitized data with background trace (blue) on bottom. The tall trace (red) on top is the first frame which goes from 0 to about 2 ½%. The middle trace is the last frame which goes from 10½% to about 13%.

Finally, the improvement in the bunch length is shown in Fig. 6. The top plots (before optimization) show a fitted ~11.5 picosecond rms bunch length compared to a final ~9.1 picosecond rms bunch length. Implementing the bunching changes brought the transmission into the damping ring up to near last year's level.

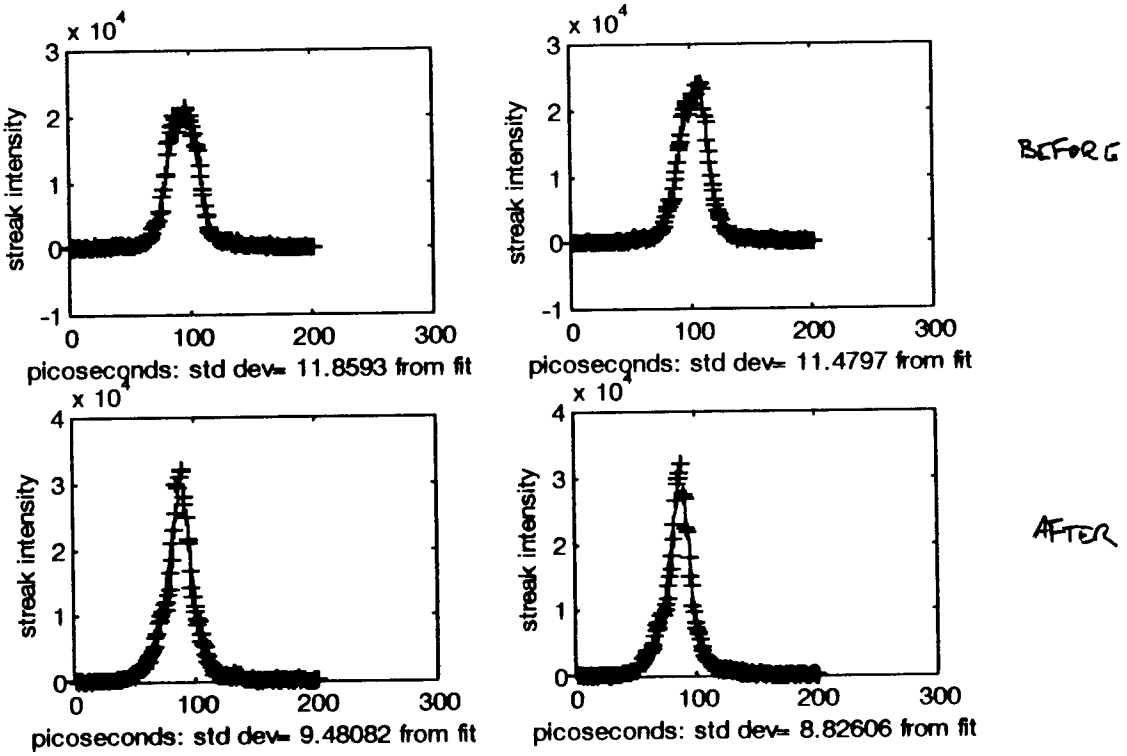

Figure 6 Top two plots are streak camera profiles of the bunch length before optimization of the phases and amplitudes fitted with an asymmetric Gaussian. The bottom two plots are representative of the bunch length after optimization.

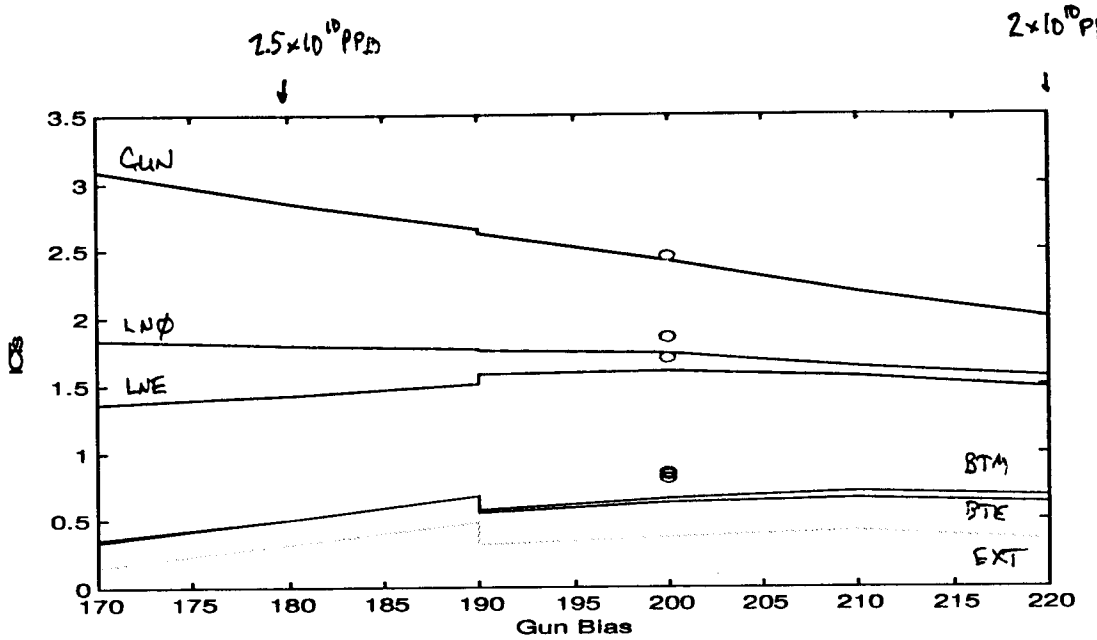

Figure 7 Gun ICT (top, blue), LN0 ICT (next , green), LNE ICT (next, red), BTM, BTE, EXT as a function of Gun Bias. Operating point shown in small circles at Gun Bias=200.

Calibration of the ICTs near the gun has been successfully achieved using a new method developed by H. Hayano and V. Vogel. The gun bias was raised to 400 volts to prevent electrons from being emitted, leaving the gun-modulator induced noise at its normal operating level. This noise is then be subtracted off as a pedestal.

There remain, however, large losses between the ICT at the end of the linac (LNE) and the middle of the BT (BTM). The mechanism for these losses is unknown.

Figure 7 shows ICTs as a function of Gun Bias. Losses mentioned above can be seen there.

05:50 STATUS: BETTER AT LNE, NOT TRANSMITTING WELL IN BT

2.95 | 1.87 | 1.69 | 0.79 | 0.77 | 0.69

LNB ↑ BTM ← lots of losses in BT

expect 85% or 2.1

typically (< 12/15/98) 1.50

06:00 SCAN FILE SAVE 98DEC15 GUNICT_ML6LX.DAT

" " " Y.DAT

06:10 [redacted]

220V	REFERENCE	1.97	1.61	1.39	0.62	0.58	0.53
180V	HIGH CURRENT	2.34	1.96	1.82	0.76	0.72	044

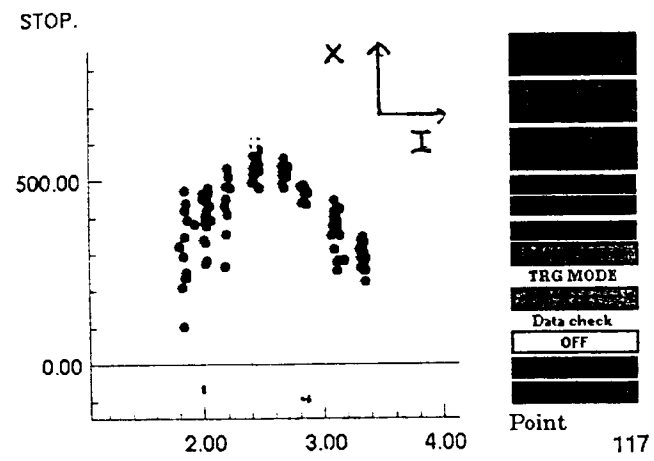

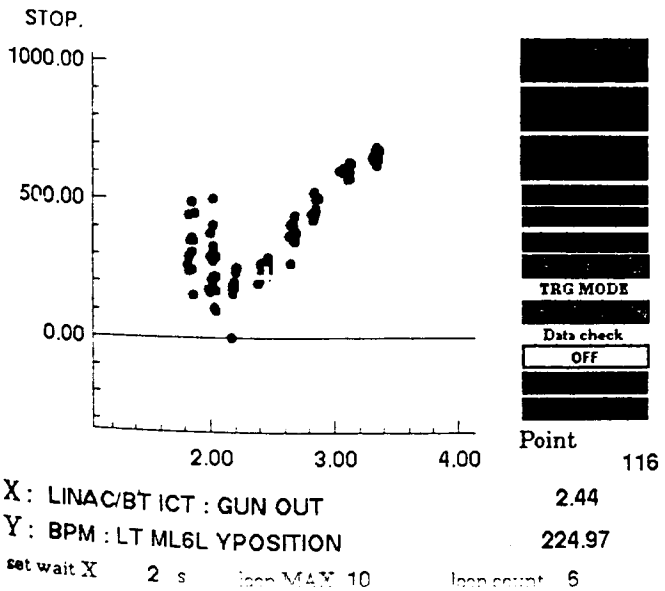

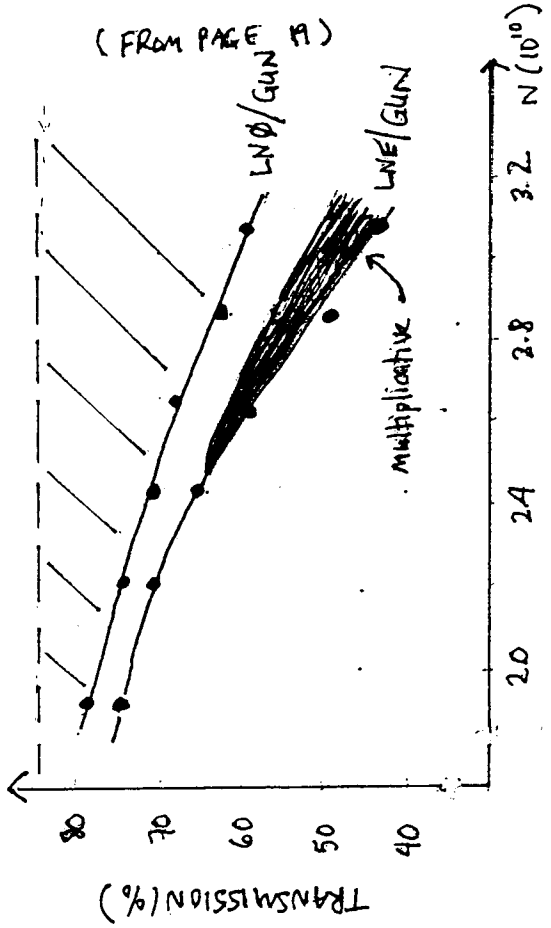

PLOTS SUGGESTIVE OF WAKEFIELD EFFECTS

Results of Recent Beam Emittance Measurements in the ATF EXT-line

M. Woodley, M. Minty, J. Turner

SLAC/KEK ISG-3
January 25, 1999

The beam sigma is obtained from the measured sigma by subtracting in quadrature the dispersive contribution $\sigma_\eta = \eta\delta_e$ and the contribution from the wire diameter, D/4. The dispersive contribution was determined by noting the change in the center position of each wire scan with a 0.1% change in the beam energy. Tables 2a and 2b summarize the data acquisition and processing. No correction was made for the pulse-to-pulse horizontal position jitter given, for reference, in column 6 of Table 2b.

4.3 Extraction Line Model

Shown in Fig. 20 are the horizontal (top) and vertical (bottom) beta functions corresponding to the extraction line optics ("EXT_addwire05", courtesy K. Kubo) which has good phase space coverage in both planes at the wire scanner locations. The Twiss parameters at each wire and the phase advance between wires are given in Table 3. In each plot of Fig. 20 are two (nearly indistinguishable) model outputs corresponding to the SLAC COMFORT-based model[8] (solid) and the online SAD model[9] (dashes).

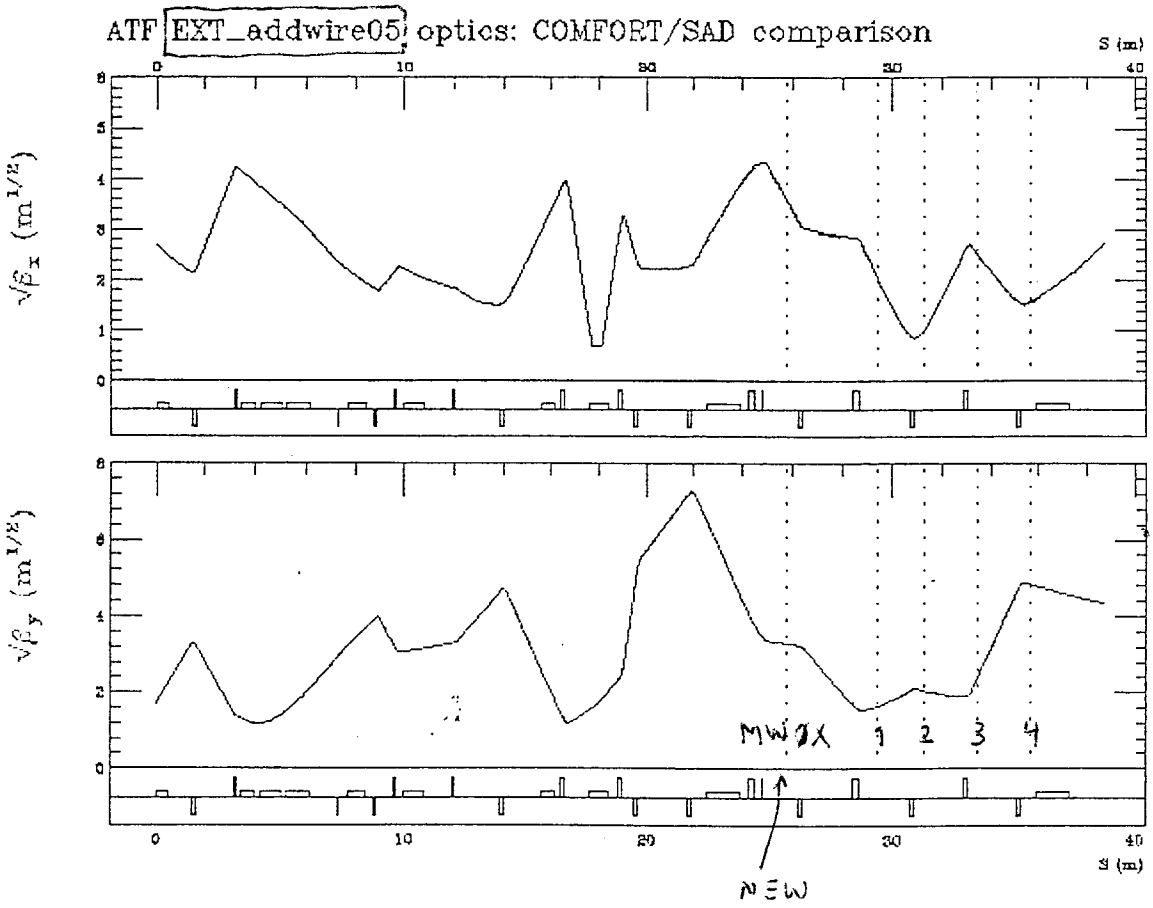

Figure 20 SAD output is dashed line, COMFORT output is solid. They coincide.

[8] P. Emma and M. Woodley, ATF-97-13 (1997)
[9] K. Oide, unpublished

ε_y (fitted) distribution by 4 or 5 wires (Simulation)

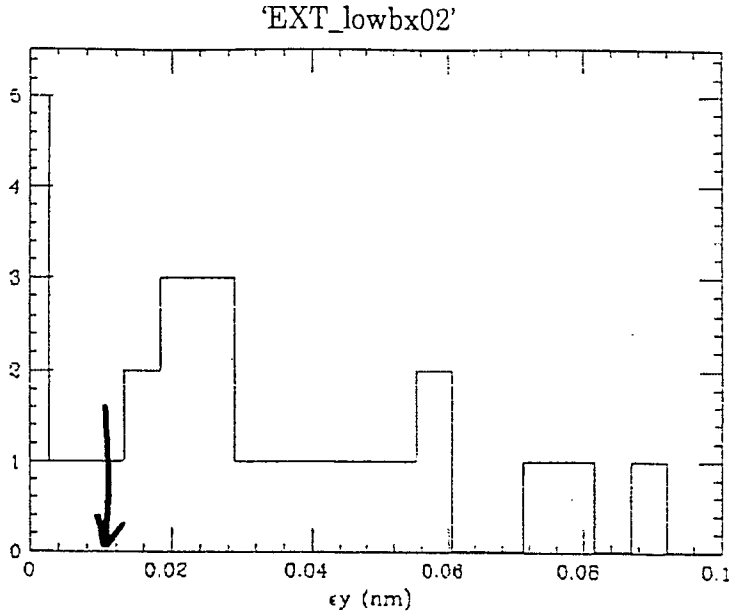

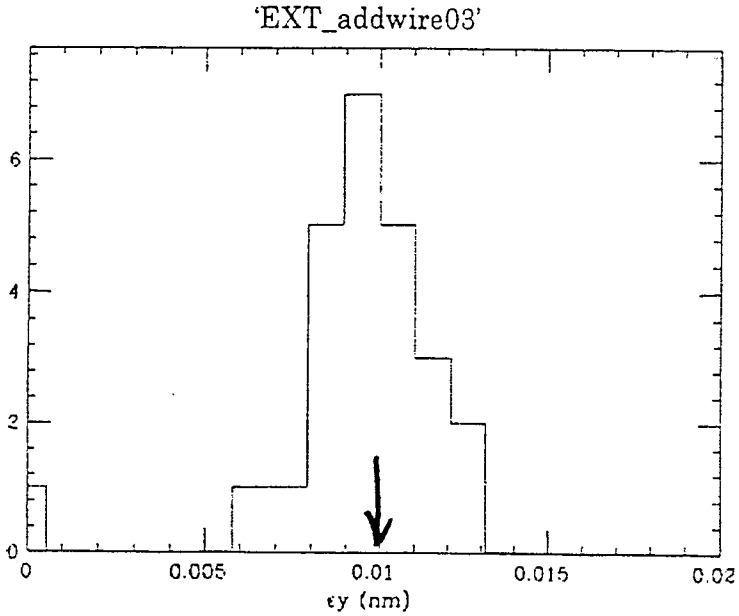

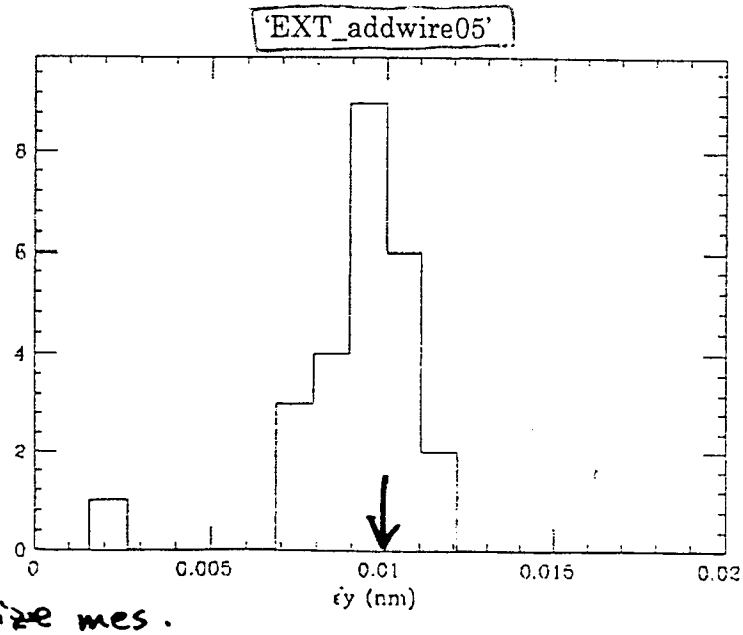

error of beam size mes.

r_1, r_2 : gaussian $\sigma = 1$

$$\text{Size(mes)} = \text{Size(real)} \times (1 + 0.1 \times r_1) + 1\mu m \times r_2$$

EXT_lowbx02 X

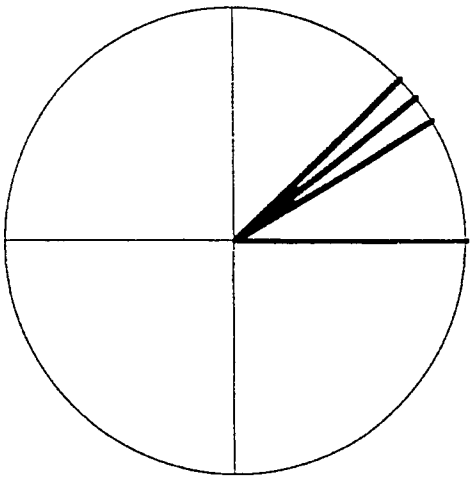

EXT_lowbx02 Y

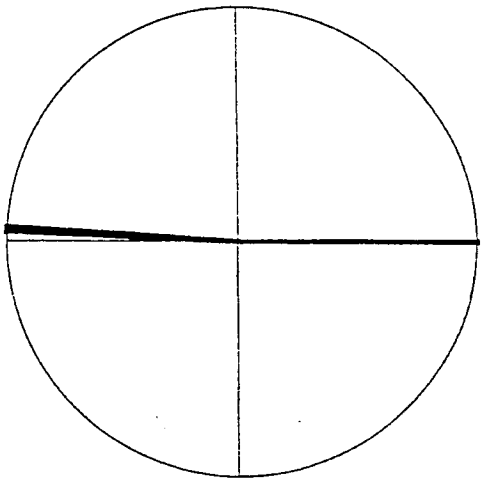

EXT_addwire03 X

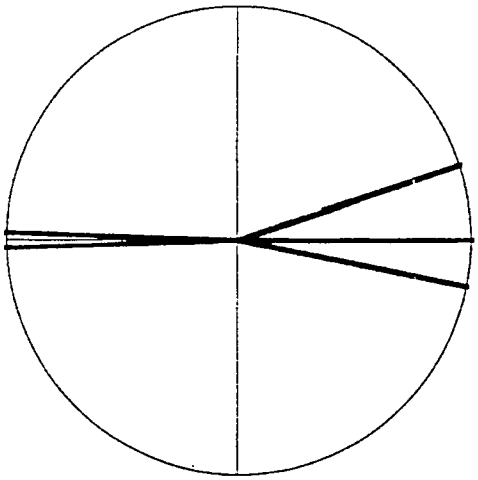

EXT_addwire03 Y

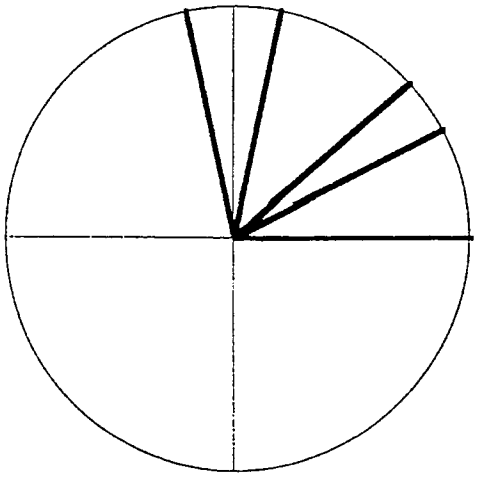

EXT_addwire05 X

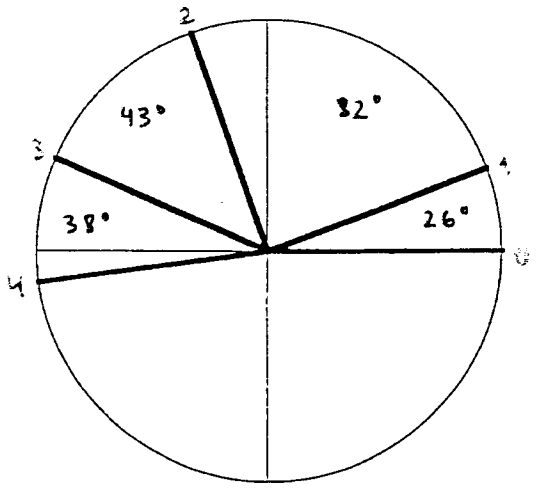

EXT_addwire05 Y

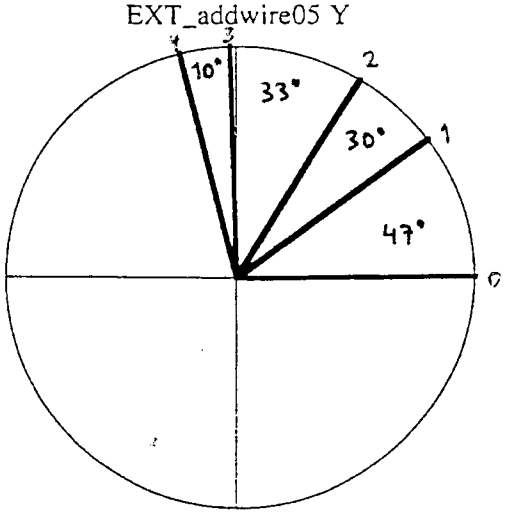

Beam Size Evaluation by Wire Scanner

$$\sigma_\beta^2 = \sigma_{meas.}^2 - \left(\eta\frac{\sigma_p}{p}\right)^2 - \left(\frac{d}{4}\right)^2$$

$\sigma_{meas.}$: Measured Beam Size at Wire Scanner

d : Wire Diameter

- RAW X AND Y DATA CORRECTED BY $\frac{1}{\sqrt{2}}$ (FOR WIRE FORK SCAN DIRECTION)
- σ_u CORRECTED BY PROJECTION OF η_x, η_y ON U-AXIS

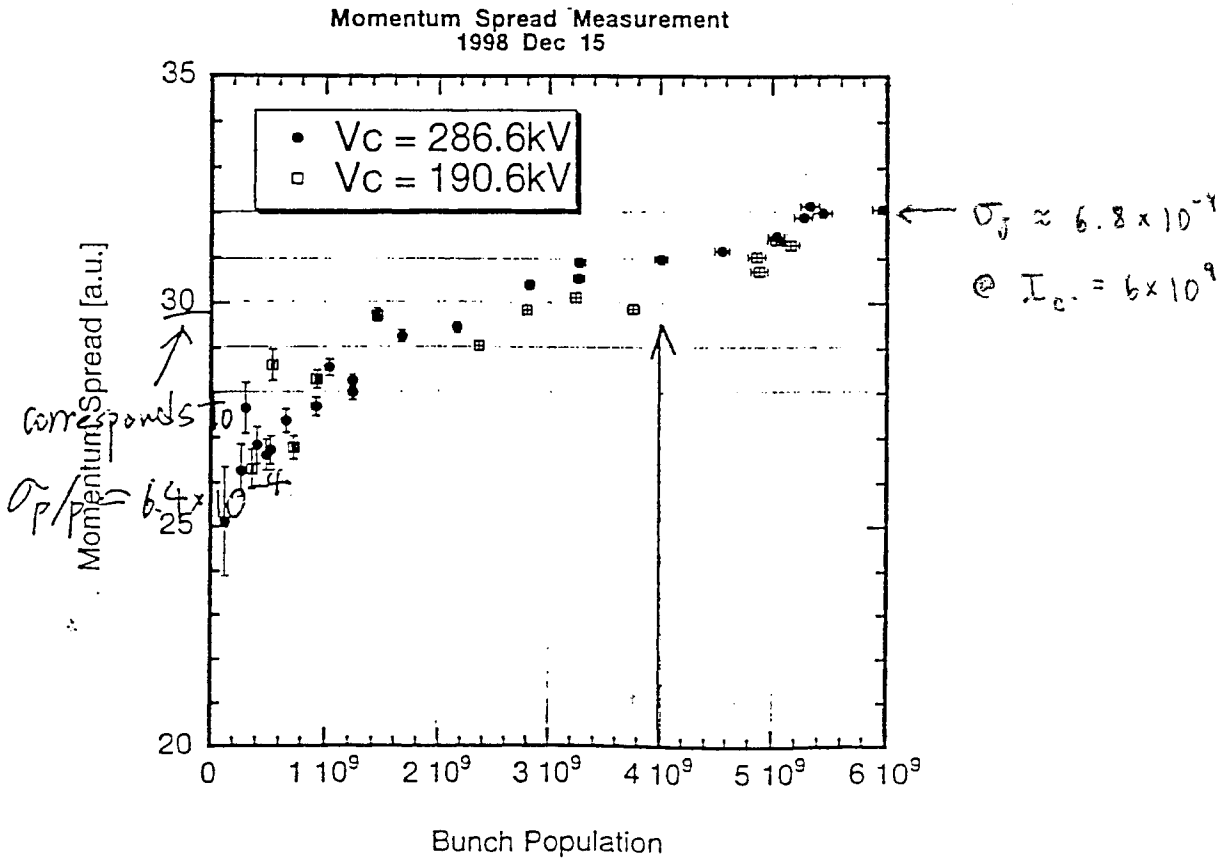

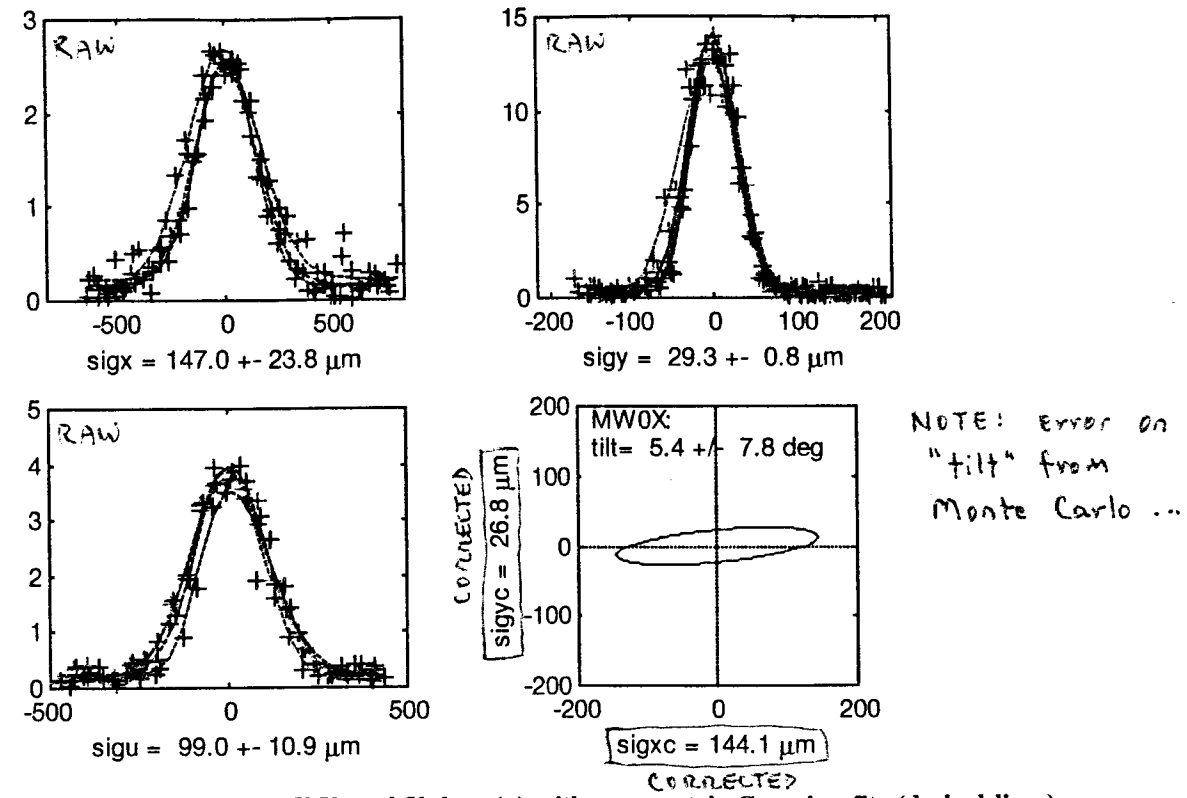

Figure 15 Wire scanner MW0X X,Y, and V data (+) with asymmetric Gaussian fits (dashed lines). Beam tilt is shown (bottom right) with the projected half-widths of the ellipse on the axes labels.

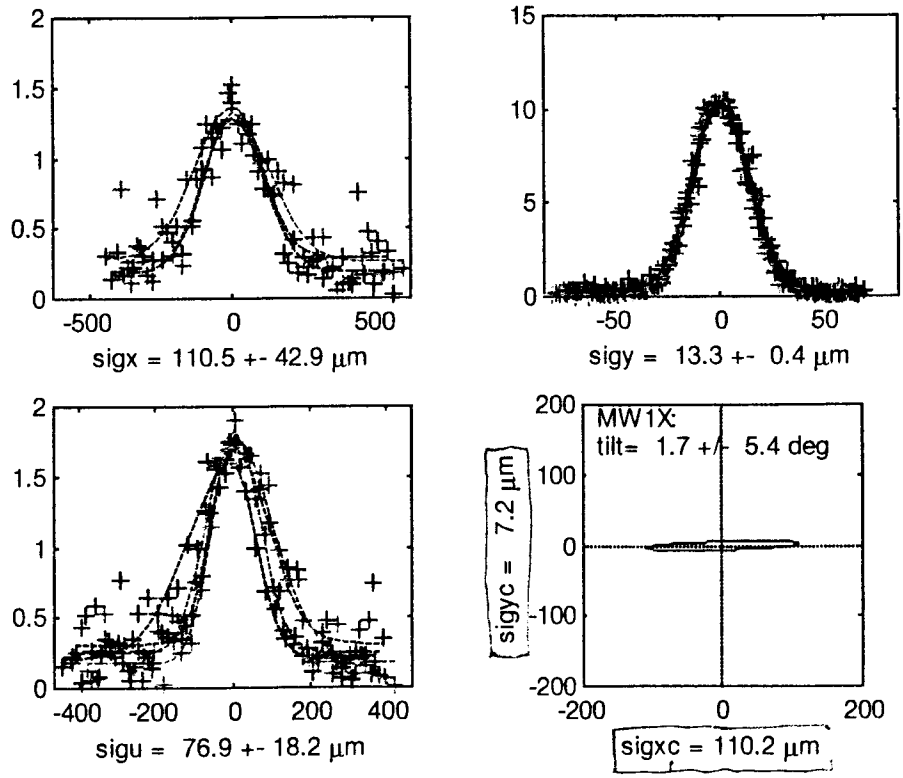

Figure 16 Wire scanner MW1X X,Y, and V data (+) with asymmetric Gaussian fits (dashed lines). Beam tilt is shown (bottom right) with the projected half-widths of the ellipse on the axes labels.

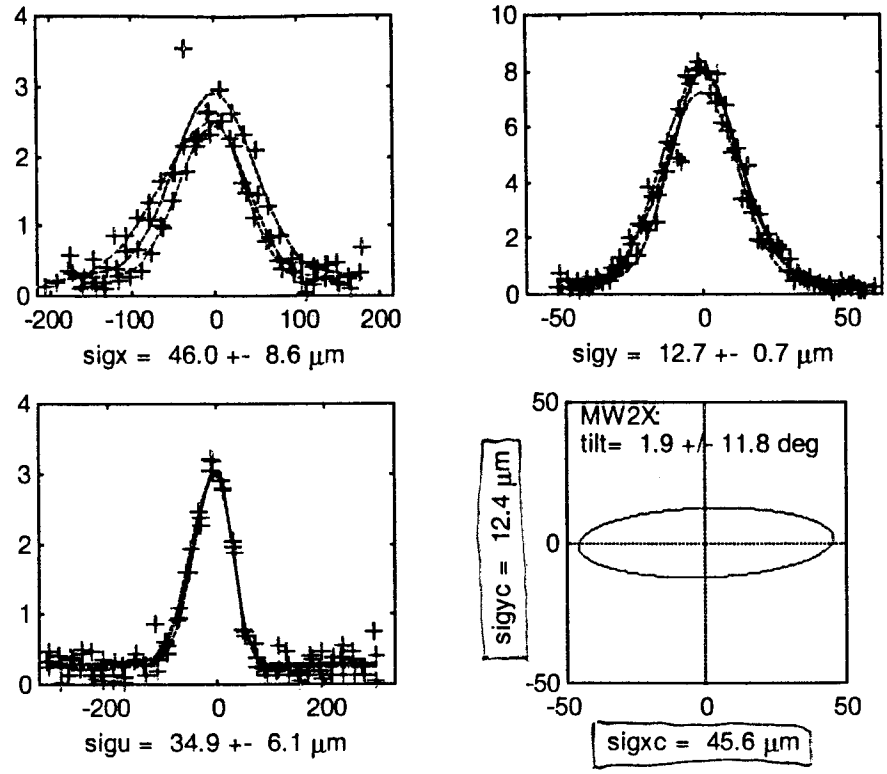

Figure 17 Wire scanner MW2X X,Y, and U data (+) with asymmetric Gaussian fits (dashed lines). Beam tilt is shown (bottom right) with the projected half-widths of the ellipse on the axes labels.

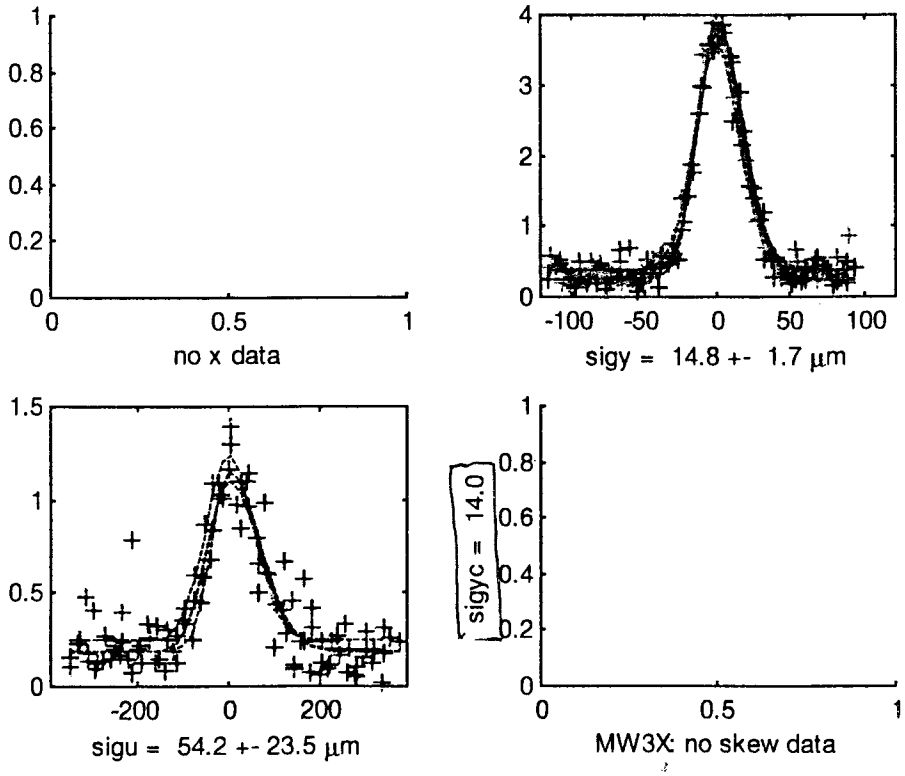

Figure 18 Wire scanner MW3 Y, and V data (+) with asymmetric Gaussian fits (dashed lines). No X data was obtained for this wire scanner.

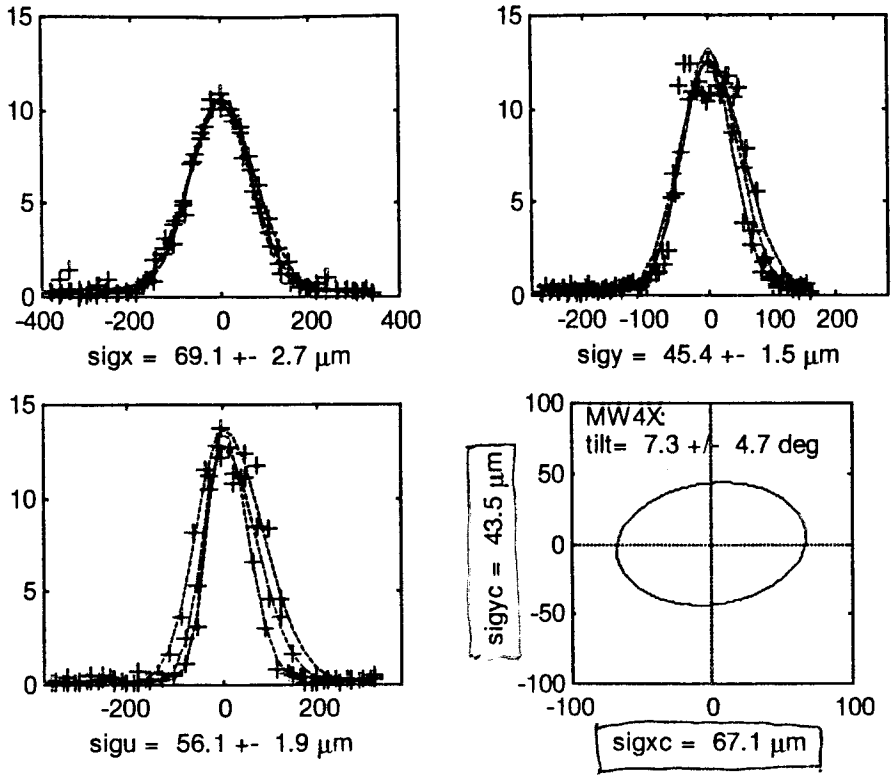

Figure 19 Wire scanner MW4X X,Y, and V data (+) with asymmetric Gaussian fits (dashed lines). Beam tilt is shown (bottom right) with the projected half-widths of the ellipse on the axes labels.

Wire	angle (deg)	N_{scan}	σ (measured) (μm)	σ (corrected) (μm)	used
MW0X.x	0	3	146.97 ± 23.76	144.09 ± 23.76	y, y
MW0X.y	90	5	29.31 ± 0.82	26.76 ± 0.82	y, y
MW0X.v	135	4	99.05 ± 10.95	94.00 ± 10.95	y, y
MW1X.x	0	3	110.47 ± 42.85	110.23 ± 42.85	y, y
MW1X.y	90	5	13.36 ± 0.37	7.18 ± 0.37	y, y
MW1X.v	135	4	76.94 ± 18.24	75.80 ± 18.24	n, n
MW2X.x	0	3	46.02 ± 8.57	34.62 ± 8.57	y, y
MW2X.y	90	3	12.80 ± 0.70	12.48 ± 0.70	y, y
MW2X.u	45	3	34.70 ± 6.08	34.14 ± 6.08	y, y
MW3X.x	0	0	no data	no data	n, n
MW3X.y	90	4	14.83 ± 1.73	14.02 ± 1.73	y, y
MW3X.v	135	3	54.17 ± 23.46	53.96 ± 23.46	y, y
MW4X.x	0	3	69.09 ± 2.69	67.05 ± 2.69	n, n
MW4X.y	90	3	45.37 ± 1.46	43.53 ± 1.46	y, n
MW4X.v	135	3	56.07 ± 1.93	53.47 ± 1.93	y, y

Table 2a summarizes the data acquisition for the emittance measurement. The columns give:

1) the wire scanner name and plane of wire,
2) the angle of orientation of the wire with respect to the horizontal axis,
3) the number of scans per wire,
4) the measured beam size (σ) with error,
5) the corrected beam sigma (see next paragraph),
6) which wires were used in the emittance calculations: y=yes, n=no; 1st column is for the 12 wire measurement, 2nd column is for the 11 wire measurement

Wire	D (μm)	η (measured) (cm)	σ_η (μm)	σ_D (μm)	jitter (measured) (μm)	tilt (measured) (deg)
MW0X.x	10	4.2	28.84	2.5	20.9	
MW0X.y	10	1.7	11.67	2.5	no data	5.4 ± 7.8
MW0X.v	10	4.2	28.65	2.5	no data	
MW1X.x	10	1.0	6.87	2.5	16.3	
MW1X.y	10	1.6	10.99	2.5	no data	1.7 ± 5.4
MW1X.v	10	1.9	12.62	2.5	no data	
MW2X.x	10	0.8	5.49	2.5	4.2	
MW2X.y	10	0.2	1.37	2.5	no data	1.4 ± 11.8
MW2X.u	10	0.7	4.86	2.5	no data	
MW3X.x	10	no data		2.5	5.5	no data
MW3X.y	10	0.6	4.12	2.5	no data	
MW3X.v	10	0.6	4.12	2.5	no data	
MW4X.x	50	1.6	10.97	12.5	no data	
MW4X.y	50	0.4	2.75	12.5	no data	7.3 ± 4.7
MW4X.v	50	1.4	9.71	12.5	no data	

Table 2b summarizes the data acquisition for the emittance measurement. The columns give:

1) the wire scanner name and plane of wire,
2) the selected wire diameter,
3) the measured dispersion function (η) at the wire,
4) the dispersive contribution to the measured σ assuming an energy spread (δ_E) of 6.8×10^{-4} (for 6×10^9 ppb[6]),
5) the measured horizontal beam jitter[7] for comparison,
6) the measured beam tilt angle with error

[6] T. Okugi, log 15 (12/15/98)
[7] T. Okugi, log 15 (12/18/98)

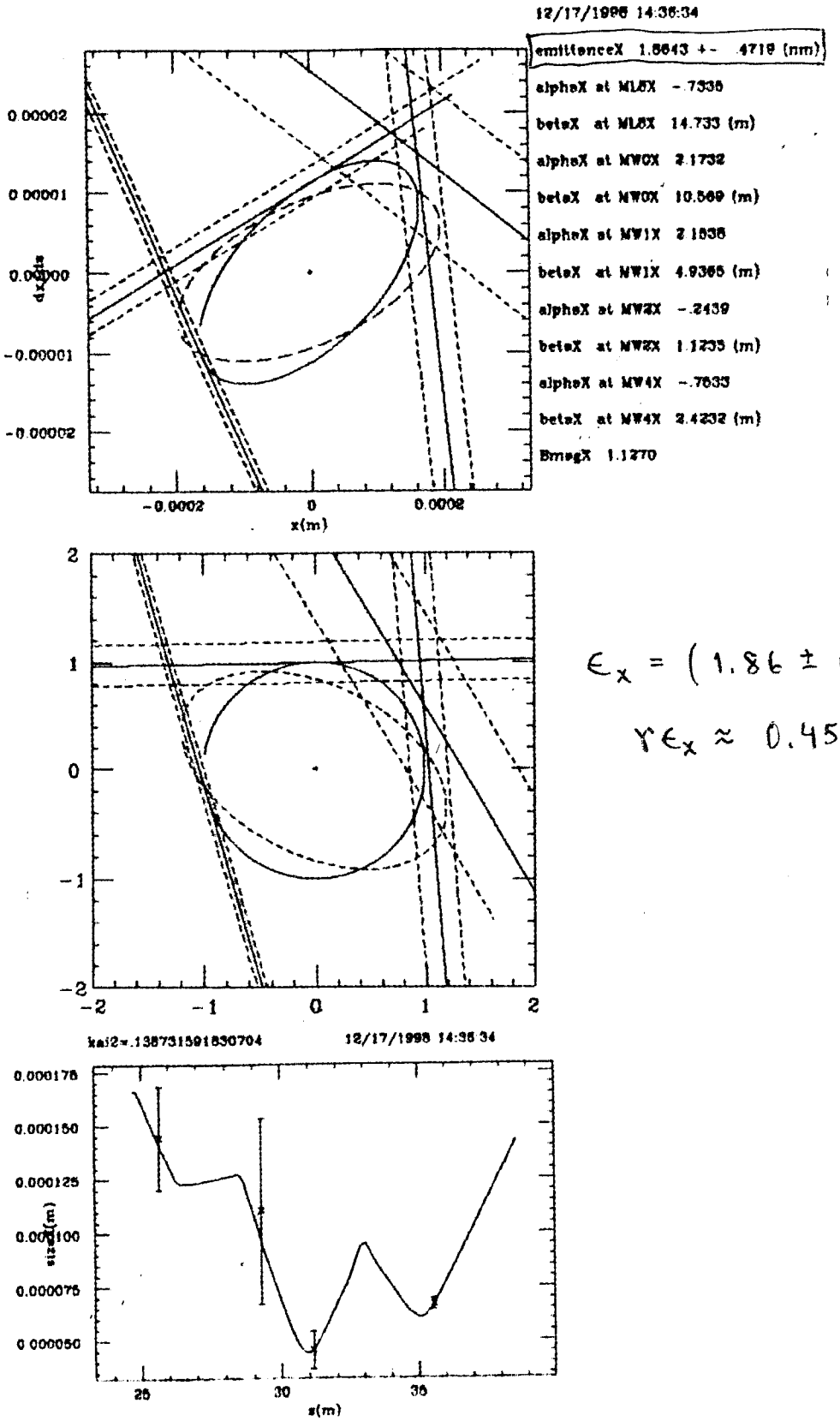

$$\epsilon_x = (1.86 \pm 0.47) \times 10^{-9}\ m$$

$$\gamma\epsilon_x \approx 0.451\ \text{SLC units}$$

Figure 21 SAD ε_x calculation using asymmetric Gaussian fits to beam sigmas.

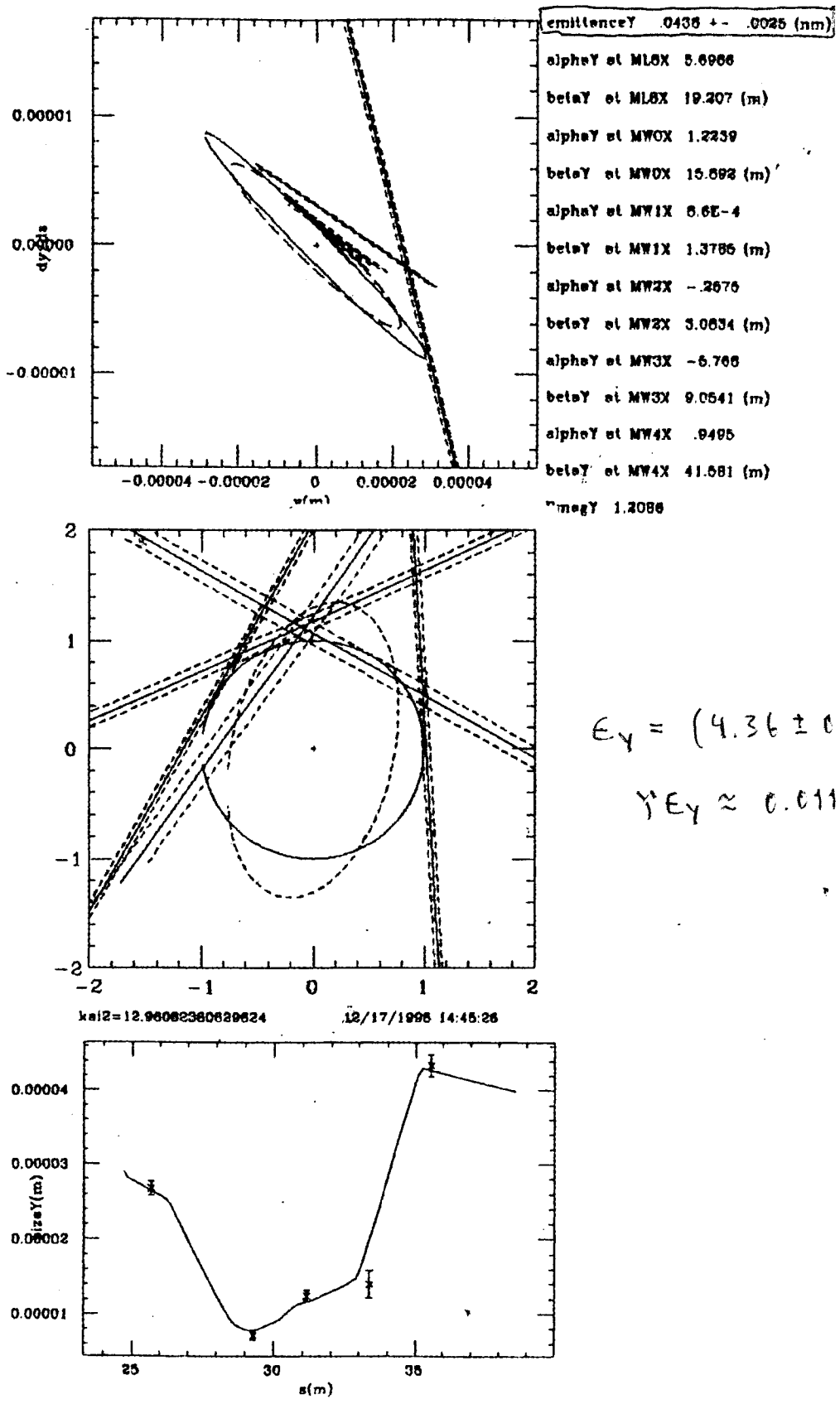

$\epsilon_y = (4.36 \pm 0.25) \times 10^{-11}$ m

$\gamma\epsilon_y \approx 0.011$ SLC units!

Figure 22 SAD ε_y calculation using asymmetric Gaussian fits to beam sigmas.

Four Dimensional Phase Space Analysis

epsilon_x = 1.733E-09 +- 4.16E-10		epsilon_y = 3.953E-11 +- 1.95E-12	
epsilon-b_x = 2.296E-09 +- 9.22E-10		epsilon-b_y = 5.044E-11 +- 2.15E-12	
Bmag_x = 1.33	+- 1.5	Bmag_y = 1.28	+- 3.07E-02
B_cos_x =-0.279	+- 0.40	B_cos_y = 0.239	+- 5.29E-02
B_sin_x =-0.594	+- 1.3	B_sin_y = 0.573	+- 6.66E-02
beta_x = 12.0		beta_y = 17.0	
alfa_x = 2.07		alfa_y = 1.25	
epsilon_1 = 1.726E-09 +- 4.17E-10		epsilon_2 = 1.533E-11 +- 5.69E-12	
beta_x = 11.9		beta_y = 18.5	
alfa_x = 2.09		alfa_y = 2.30	
B_11 =-0.115		B_12 = 8.081E-02	
B_21 = 0.152		B_22 =-7.371E-02	
tr(BB') = 4.826E-02		det B =-3.844E-03	

$\frac{\epsilon_Y}{\epsilon_X} \approx 2.3\%$

$\frac{\epsilon_Y}{\epsilon_X} \approx 0.9\%$

chi^2/dof = 17.5

wire	angle/deg	Tmit/E10	sigma measured	sigma fit
MW0X.x	0	0.60	144.09 +- 23.756	144.09
MW1X.x	0	0.60	110.23 +- 42.852	110.23
MW2X.x	0	0.60	45.623 +- 8.5721	45.623
MW0X.y	90	0.60	26.765 +- 0.81613	25.949
MW1X.y	90	0.60	7.1781 +- 0.36648	7.5284
MW2X.y	90	0.60	12.475 +- 0.69764	10.523
MW3X.y	90	0.60	14.023 +- 1.7259	18.470
MW0X.v	135	0.60	94.003 +- 10.945	94.004
MW2X.u	45	0.60	34.142 +- 6.0841	34.142
MW3X.v	135	0.60	53.957 +- 23.457	53.957
MW4X.v	135	0.60	53.469 +- 1.9334	53.469

11 σ's
(1 D.O.F.)

Four Dimensional Phase Space Analysis

epsilon_x = 1.733E-09 +- 4.16E-10		epsilon_y = 4.106E-11 +- 1.80E-12	
epsilon-b_x = 2.296E-09 +- 9.22E-10		epsilon-b_y = 5.363E-11 +- 2.15E-12	
Bmag_x = 1.33	+- 1.5	Bmag_y = 1.31	+- 3.07E-02
B_cos_x =-0.279	+- 0.40	B_cos_y = 0.198	+- 5.29E-02
B_sin_x =-0.594	+- 1.3	B_sin_y = 0.612	+- 6.66E-02
beta_x = 12.0		beta_y = 16.9	
alfa_x = 2.07		alfa_y = 1.31	
epsilon_1 = 1.727E-09 +- 4.17E-10		epsilon_2 = 1.403E-11 +- 7.24E-12	
beta_x = 12.0		beta_y = 19.8	
alfa_x = 2.09		alfa_y = 2.68	
B_11 =-0.144		B_12 = 8.142E-02	
B_21 = 0.166		B_22 =-7.150E-02	
tr(BB') = 5.996E-02		det B =-3.224E-03	

$\frac{\epsilon_Y}{\epsilon_X} \approx 2.4\%$ ⟷

$\frac{\epsilon_Y}{\epsilon_X} \approx 0.8\%$ ⟷

chi^2/dof = 9.95

wire	angle/deg	Tmit/E10	sigma measured	sigma fit
MW0X.x	0	0.60	144.09 +- 23.756	144.09
MW1X.x	0	0.60	110.23 +- 42.852	110.23
MW2X.x	0	0.60	45.623 +- 8.5721	45.623
MW0X.y	90	0.60	26.765 +- 0.81613	26.306
MW1X.y	90	0.60	7.1781 +- 0.36648	7.4122
MW2X.y	90	0.60	12.475 +- 0.69764	11.046
MW3X.y	90	0.60	14.023 +- 1.7259	19.501
MW4X.y	90	0.60	43.531 +- 1.4614	42.007
MW0X.v	135	0.60	94.003 +- 10.945	94.004
MW2X.u	45	0.60	34.142 +- 6.0841	34.142
MW3X.v	135	0.60	53.957 +- 23.457	53.957
MW4X.v	135	0.60	53.469 +- 1.9334	53.469

12 σ's
(2 D.O.F.)

4D Emittance Measurement

$$\sigma = \begin{pmatrix} \sigma_{11} & \sigma_{12} & \sigma_{13} & \sigma_{14} \\ \sigma_{21} & \sigma_{22} & \sigma_{23} & \sigma_{24} \\ \sigma_{31} & \sigma_{32} & \sigma_{33} & \sigma_{34} \\ \sigma_{41} & \sigma_{42} & \sigma_{43} & \sigma_{44} \end{pmatrix}$$

$$\sigma_i = R_i \sigma_0 R_i^T$$

$$\vec{\sigma}_0 \equiv \begin{pmatrix} \sigma_{11_0} & \sigma_{21_0} & \sigma_{31_0} & \sigma_{41_0} & \sigma_{22_0} & \sigma_{32_0} & \sigma_{42_0} & \sigma_{33_0} & \sigma_{43_0} & \sigma_{44_0} \end{pmatrix}^T$$

$$\sigma_x^{\,2} = \sigma_{11}$$
$$\sigma_y^{\,2} = \sigma_{33}$$
$$\sigma_u^{\,2} = \sigma_{31} + \frac{1}{2}(\sigma_{11} + \sigma_{33}) \quad *$$

$$\vec{\sigma}_i^m \equiv \begin{pmatrix} \sigma_{x_i}^{\,2} \\ \sigma_{y_i}^{\,2} \\ \sigma_{u_i}^{\,2} \end{pmatrix} = M \begin{pmatrix} \sigma_{11_i} \\ \sigma_{33_i} \\ \sigma_{31_i} \end{pmatrix}, \quad M = \begin{pmatrix} 1 & 0 & 0 \\ 0 & 1 & 0 \\ \frac{1}{2} & \frac{1}{2} & 1 \end{pmatrix}$$

$$\vec{\sigma}_i^m = M P_i \vec{\sigma}_0$$

$$P = \begin{pmatrix} R_{11}^{\,2} & R_{31}^{\,2} & R_{11}R_{31} \\ 2R_{11}R_{12} & 2R_{31}R_{32} & R_{12}R_{31} + R_{11}R_{32} \\ 2R_{11}R_{13} & 2R_{31}R_{33} & R_{13}R_{31} + R_{11}R_{33} \\ 2R_{11}R_{14} & 2R_{31}R_{34} & R_{14}R_{31} + R_{11}R_{34} \\ R_{12}^{\,2} & R_{32}^{\,2} & R_{12}R_{32} \\ 2R_{12}R_{13} & 2R_{32}R_{33} & R_{13}R_{32} + R_{12}R_{33} \\ 2R_{12}R_{14} & 2R_{32}R_{34} & R_{14}R_{32} + R_{12}R_{34} \\ R_{13}^{\,2} & R_{33}^{\,2} & R_{13}R_{33} \\ 2R_{13}R_{14} & 2R_{33}R_{34} & R_{14}R_{33} + R_{13}R_{34} \\ R_{14}^{\,2} & R_{34}^{\,2} & R_{14}R_{34} \end{pmatrix}^T$$

* IN GENERAL, $\sigma_w^{\,2} = \sigma_{11}\cos^2\theta_w + \sigma_{33}\sin^2\theta_w + \sigma_{31}\sin 2\theta_w$

4D Emittance Measurement (cont.)

$$P_{uncoupled} = \begin{pmatrix} R_{11}^{\,2} & 0 & 0 \\ 2R_{11}R_{12} & 0 & 0 \\ 0 & 0 & R_{11}R_{33} \\ 0 & 0 & R_{11}R_{34} \\ R_{12}^{\,2} & 0 & 0 \\ 0 & 0 & R_{12}R_{33} \\ 0 & 0 & R_{12}R_{34} \\ 0 & R_{33}^{\,2} & 0 \\ 0 & 2R_{33}R_{34} & 0 \\ 0 & R_{34}^{\,2} & 0 \end{pmatrix}^T$$

Given at the i^{th} measurement location: $\sigma_{x_i} \pm \delta\sigma_{x_i}$, $\sigma_{y_i} \pm \delta\sigma_{y_i}$, $\sigma_{u_i} \pm \delta\sigma_{u_i}$

$$\vec{\sigma}_i^{\,m} = \begin{pmatrix} \sigma_{x_i}^{\,2} \\ \sigma_{y_i}^{\,2} \\ \sigma_{u_i}^{\,2} \end{pmatrix}, \quad D_i \equiv \begin{pmatrix} \dfrac{1}{2\sigma_{x_i}\delta\sigma_{x_i}} & 0 & 0 \\ 0 & \dfrac{1}{2\sigma_{y_i}\delta\sigma_{y_i}} & 0 \\ 0 & 0 & \dfrac{1}{2\sigma_{u_i}\delta\sigma_{u_i}} \end{pmatrix}$$

$$\vec{s} \equiv \begin{pmatrix} D_1\vec{\sigma}_1^{\,m} \\ \vdots \\ D_N\vec{\sigma}_N^{\,m} \end{pmatrix}, \quad Q \equiv \begin{pmatrix} D_1 M P_1 \\ \vdots \\ D_N M P_N \end{pmatrix}$$

$$\vec{s} = Q\vec{\sigma}_0 \quad \Rightarrow \quad Q^T\vec{s} = \left(Q^TQ\right)\vec{\sigma}_0 \quad \Rightarrow \quad \boxed{\left(Q^TQ\right)^{-1}Q^T\vec{s} = \vec{\sigma}_0}$$

$$C \equiv \text{covariance matrix} = \left(Q^TQ\right)^{-1}$$

$$\delta\sigma_{0_j} = \sqrt{C_{jj}} \quad , \quad \chi^2 = \vec{s}^{\,T}\vec{s} - \vec{s}^{\,T}\left(Q\,C\,Q^T\right)\vec{s}$$

Intrinsic Emittance From Measured 4×4 Beam Matrix[1]

$$\sigma_m = \begin{pmatrix} \sigma_{11} & \sigma_{12} & \sigma_{13} & \sigma_{14} \\ \sigma_{21} & \sigma_{22} & \sigma_{23} & \sigma_{24} \\ \sigma_{31} & \sigma_{32} & \sigma_{33} & \sigma_{34} \\ \sigma_{41} & \sigma_{42} & \sigma_{43} & \sigma_{44} \end{pmatrix}_m \quad , \quad \bar{\sigma} \equiv \begin{pmatrix} \varepsilon_1 & 0 & 0 & 0 \\ 0 & \varepsilon_1 & 0 & 0 \\ 0 & 0 & \varepsilon_2 & 0 \\ 0 & 0 & 0 & \varepsilon_2 \end{pmatrix} = \bar{R}\,\sigma_m \bar{R}^T$$

Note: σ_m **must** be *positive definite*

$$S \equiv \begin{pmatrix} 0 & -1 & 0 & 0 \\ 1 & 0 & 0 & 0 \\ 0 & 0 & 0 & -1 \\ 0 & 0 & 1 & 0 \end{pmatrix} \quad , \quad RSR^T = R^T SR = S$$

$$[\bar{\sigma} S]^2 = \begin{pmatrix} -\varepsilon_1^2 & 0 & 0 & 0 \\ 0 & -\varepsilon_1^2 & 0 & 0 \\ 0 & 0 & -\varepsilon_2^2 & 0 \\ 0 & 0 & 0 & -\varepsilon_2^2 \end{pmatrix}, \quad [\bar{\sigma} S]^4 = \begin{pmatrix} \varepsilon_1^4 & 0 & 0 & 0 \\ 0 & \varepsilon_1^4 & 0 & 0 \\ 0 & 0 & \varepsilon_2^4 & 0 \\ 0 & 0 & 0 & \varepsilon_2^4 \end{pmatrix}$$

$$\mathrm{tr}\,(\bar{\sigma} S) = \mathrm{tr}\,(\bar{R}\,\sigma_m \bar{R}^T S) = \mathrm{tr}\,(\sigma_m \bar{R}^T S \bar{R}) = \mathrm{tr}\,(\sigma_m S)$$

$$\mathrm{tr}\,([\bar{\sigma} S]^2) = \mathrm{tr}\,([\sigma_m S]^2), \quad \mathrm{tr}\,([\bar{\sigma} S]^4) = \mathrm{tr}\,([\sigma_m S]^4)$$

$$t_2 \equiv \mathrm{tr}\,([\bar{\sigma} S]^2) = -2(\varepsilon_1^2 + \varepsilon_2^2) \;\Rightarrow\; \varepsilon_1^2 = -\frac{t_2}{2} - \varepsilon_2^2 \;\Rightarrow\; \varepsilon_1^4 = \frac{t_2^2}{4} + t_2 \varepsilon_2^2 + \varepsilon_2$$

$$t_4 \equiv \mathrm{tr}\,([\bar{\sigma} S]^4) = 2(\varepsilon_1^4 + \varepsilon_2^4) \;\Rightarrow\; t_4 = 2\left(\frac{t_2^2}{4} + 2\varepsilon_2^4 + t_2 \varepsilon_2^2\right) \;\Rightarrow\; 4\varepsilon_2^4 + 2t_2 \varepsilon_2^2 + \frac{t_2^2}{2} - t_4 = 0$$

$$\boxed{\varepsilon_1^2 = \frac{-t_2 + \sqrt{-t_2^2 + 4t_4}}{4}, \quad \varepsilon_2^2 = \frac{-t_2 - \sqrt{-t_2^2 + 4t_4}}{4}}$$

[1] From Stefan Fartouk (Saclay) via Paul Emma.

ATF EXT-line 4D Emittance Measurement (16-DEC-98)

The measured beam matrix (12 measured σ's, least-squares fit) was:

$$\sigma_{measured} = \begin{bmatrix} 2.076\times10^{-8} & -3.588\times10^{-9} & 1.890\times10^{-9} & -3.566\times10^{-11} \\ -3.588\times10^{-9} & 7.647\times10^{-10} & -1.410\times10^{-10} & -3.214\times10^{-12} \\ 1.890\times10^{-9} & -1.410\times10^{-10} & 6.920\times10^{-10} & -5.369\times10^{-11} \\ -3.566\times10^{-11} & -3.214\times10^{-12} & -5.369\times10^{-11} & 6.602\times10^{-12} \end{bmatrix}$$

Expressed in TRANSPORT notation:

$$\begin{array}{llll} \sqrt{\sigma_{11}} & & 144.086 \ \mu m & \\ \sqrt{\sigma_{22}} \quad r_{21} & & 27.654 \ \mu rad & -0.9005 \\ \sqrt{\sigma_{33}} \quad r_{31} \quad r_{32} & = & 26.306 \ \mu m & 0.4986 \quad -0.1938 \\ \sqrt{\sigma_{44}} \quad r_{41} \quad r_{42} \quad r_{43} & & 2.569 \ \mu rad & -0.0963 \quad -0.0452 \quad -0.7944 \end{array}$$

where $$r_{ij} \equiv \frac{\sigma_{ij}}{\sqrt{\sigma_{ii}\sigma_{jj}}}$$

The projected emittances are:

$$\varepsilon_x = 1.733\times10^{-9}\,\text{m} \quad , \quad \varepsilon_y = 4.106\times10^{-11}\,\text{m}$$

The intrinsic emittances[2] are:

$$\varepsilon_1 = 1.727\times10^{-9}\,\text{m} \quad , \quad \varepsilon_2 = 1.403\times10^{-11}\,\text{m}$$

[2] Computed by both the Bill Spence "EMIT4D" program and the Stefan Fartouk method.

Correction of Measured Coupling

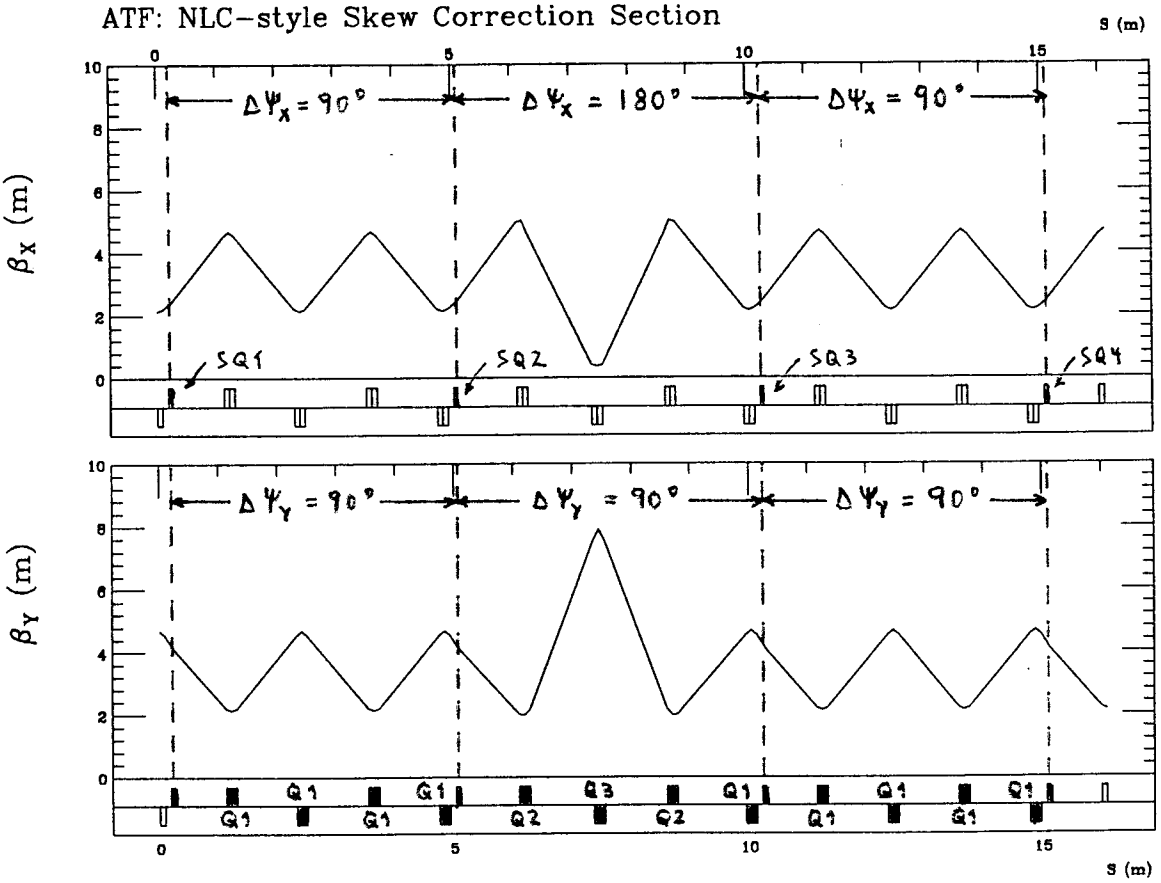

Shown above is an NLC-style skew correction system[3] adapted for ATF. The system consists of 12 Hitachi Type 4 quadrupoles, which comprise the FODO lattice, plus 4 Tokin 6 cm skew quadrupoles. The system is approximately 15 meters long. For a beam energy of 1.2386 GeV, the FODO quadrupole strengths would be:

Skew Correction Section FODO quads: Hitachi Type 4
(I_{MAX} = 200 amps)

Family	Quantity	$K1_{SAD}$	I (amps)
Q1	9	0.6665	60.3
Q2	2	1.0673	97.0
Q3	1	0.8967	81.3

[3] See the NLC Design Report (SLAC Report 474), pp. 666-668.

Correction of Measured Coupling (cont.)

Taking the beam matrix measured in the ATF EXT-line (16-DEC-1998) as input, the skew quadrupole strengths needed to correct the measured coupling terms ($r_{31}, r_{32}, r_{41}, r_{42}$) to zero are:

Skew Correction Section skew quads: Tokin 6 cm
(I_{MAX} = 140 amps)

Magnet	Quantity	$K1_{SAD}$	I (amps)
SQ1	1	0.0187	5.5
SQ2	1	0.1121	35.4
SQ3	1	0.0325	9.8
SQ4	1	0.0775	24.1

The corrected beam matrix (in TRANSPORT notation) is:

$$\begin{array}{lll} \sqrt{\sigma_{11}} & & 160.064\ \mu\text{m} \\ \sqrt{\sigma_{22}} & r_{21} & 33.141\ \mu\text{rad} \\ \sqrt{\sigma_{33}} & r_{31}\ r_{32} & 10.999\ \mu\text{m} \\ \sqrt{\sigma_{44}} & r_{41}\ r_{42}\ r_{43} & 3.386\ \mu\text{rad} \end{array} = \begin{array}{llll} & & & \\ -0.9455 & & & \\ 0.0 & 0.0 & & \\ 0.0 & 0.0 & 0.9264 & \end{array}$$

The corrected projected emittances are:

$$\varepsilon_x = 1.727 \times 10^{-9}\,\text{m} \quad , \quad \varepsilon_y = 1.402 \times 10^{-11}\,\text{m}$$

3. Comparison of Vertical Emittance Measurements

One of the primary challenges at the ATF is demonstrating the ability to measure extremely small vertical beam emittances of a few picometer-radians. At the ATF there are two direct measurements of the vertical emittance: an upper bound is determined using novel interferometric techniques[1] using emitted synchrotron radiation in the damping ring, and an absolute measurement is made with conventional wire scanners[2] in the extraction line.

In this experiment we measured the beam emittance using both methods while varying the vertical beam size by approaching a coupling resonance. With absolute emittance measurements, a comparison of the two diagnostic methods may be used to infer any additive contributions to the emittance generated in the extraction channel or find systematic errors in the diagnostics themselves. With apriori knowledge that the interferometer gives an upper bound on the emittance, the comparison may be useful in estimating the amount by which the emittance may be overestimated due to degradation of the spatial coherence due possible beam tails or optical component imperfections, for example.

For comparison of the measured vertical emittances, 5 measurements were made for each set of tunes:

1) a 5-wire vertical emittance measurement in the extraction line with 3 scans per wire,
2) a single scan of each wire with a 0.1% relative energy offset to measure the vertical dispersion at each wire,
3) 10 samples of the vertical beam size obtained using the new (courtesy H. Hayano) online fitting of the interferometer, and
4) calibration data consisting of beta function measurements (determined by changing the trim coil current in the two nearby quadrupoles QM4R.2 and QM5R.2 by ± 2.5 Amperes and measuring the shift in betatron tune), and
5) a dispersion measurement made by changing the damping ring rf frequency by ± 5 kHz and observing the change in orbit.

The latter 2 measurements determine the Twiss β and η parameters at the radiation emission point.

Before the measurement, the coupling resonance was first approached as shown in Figure 9. In Fig. 10 the spot size as measured by the interferometer is shown as a function of tune difference $\delta\nu$. The raw data are given in the top plot while the lower plot shows the square of the beam size along with the curve[3]:

$$\sigma_y^2 = \beta_y \varepsilon_x \frac{2\kappa^2}{3\kappa^2 + (\delta\upsilon)^2}$$

where κ is the coupling coefficient which is taken to be 0.032 from Fig. 9, β_y is the vertical beta function at the source emission point, and ε_x is the uncoupled horizontal beam emittance. Here we set $\beta_y \varepsilon_x = 2600 \ \ m^2 r$ and take β_y to be fixed, which is reasonable for small tune variations.

[1] T. Mitsuhashi and T. Naito, "Measurement of Beam Size at the ATF Damping Ring with the SR Interferometer", EPAC'98, ATF-98-17 (1998)

[2] S. Kashiwagi et al "Diagnosis of the Low Emittance Beam in the ATF DR Extraction Line", ATF-98-20

[3] F. Zimmermann et al "Vertical Emittance Studies at the ATF Damping Ring", SLAC/AP-113 (1998)

measured bea
for dispersion
the online S.
plot.

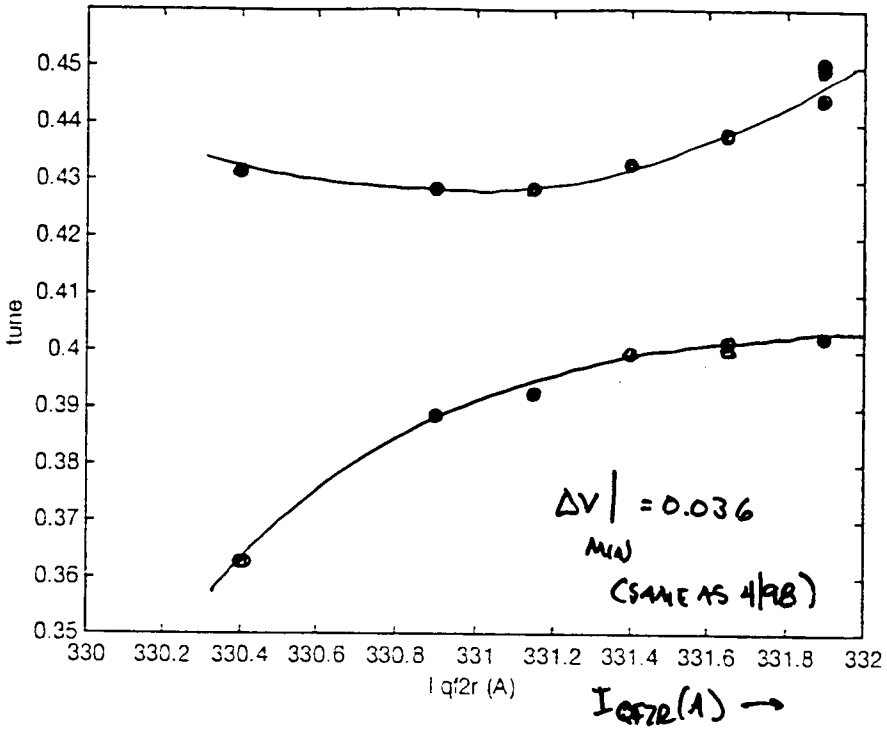

Figure 9 Measurement of coupling resonance width showing measured betatron tunes versus quadrupole current.

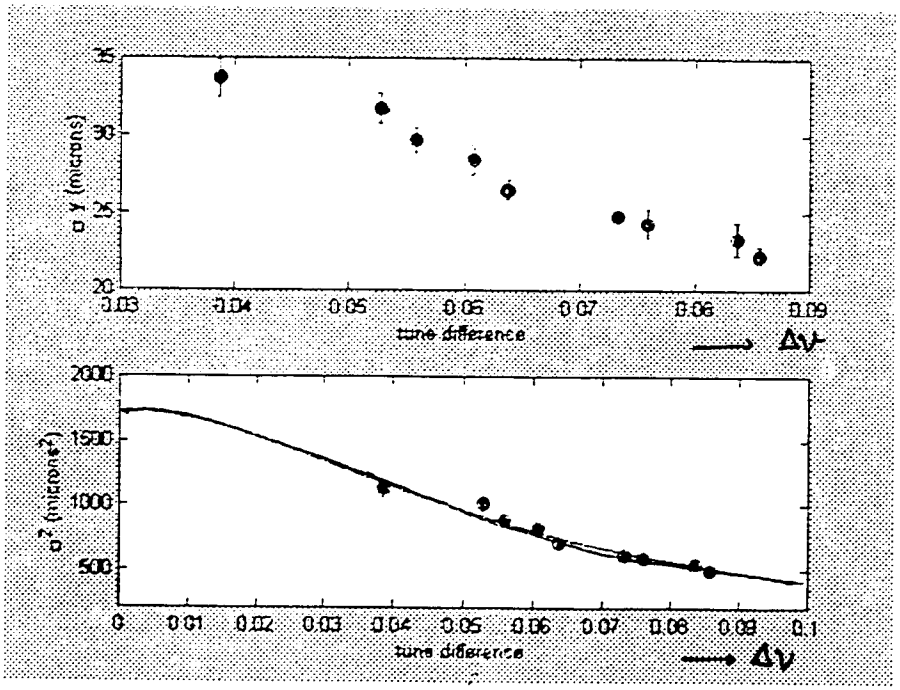

Figure 10 Beam size measurements near the coupling resonance. The top plot shows the raw data while the bottom plot shows the square of the beam size (note different scales) along with theoretical estimate (see text).

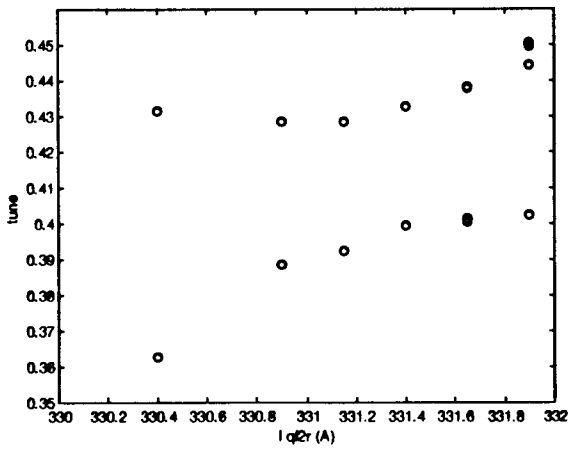

Figure 9 Measurement of coupling resonance width showing measured betatron tunes versus quadrupole current.

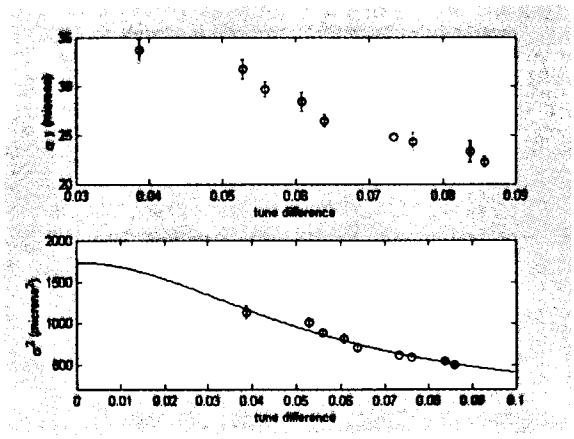

Figure 10 Beam size measurements near the coupling resonance. The top plot shows the raw data while the bottom plot shows the square of the beam size (note different scales) along with theoretical estimate (see text).

Shown in the next three figures are the extraction line emittance measurements analyzed online using SAD which includes dispersion correction at the wires. Respectively are shown the emittances under nominal conditions (Fig. 11), with a tune separation of 0.0558 ± 0.0014 (Fig. 12), and with a tune separation of 0.0709 ± 0.0012 (Fig. 13). These tune separations were selected to span the range of good visibility (vertical beam sizes ranging from about 15 to 30 microns).

In Figs. 11-13 the emittances are plotted in y-y' space (top) and normalized phase space (middle). The measured beam sigmas, after correcting for dispersion, are given together with the online SAD model in the bottom plot.

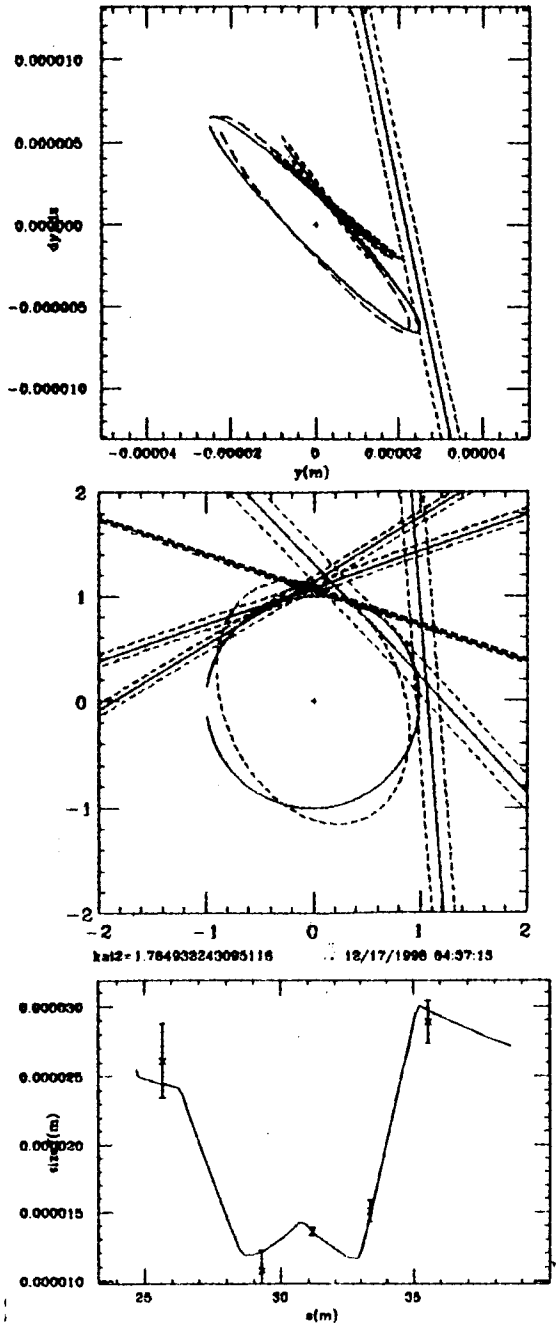

Figure 11 Extraction line Y emittance measurement under nominal conditions (ν_x=0.2048+/-0.0005, ν_y=0.7410+/-0.0007): BMAG=1.07, and $\varepsilon_y = 46.6 \pm 3.3$ pm-r.

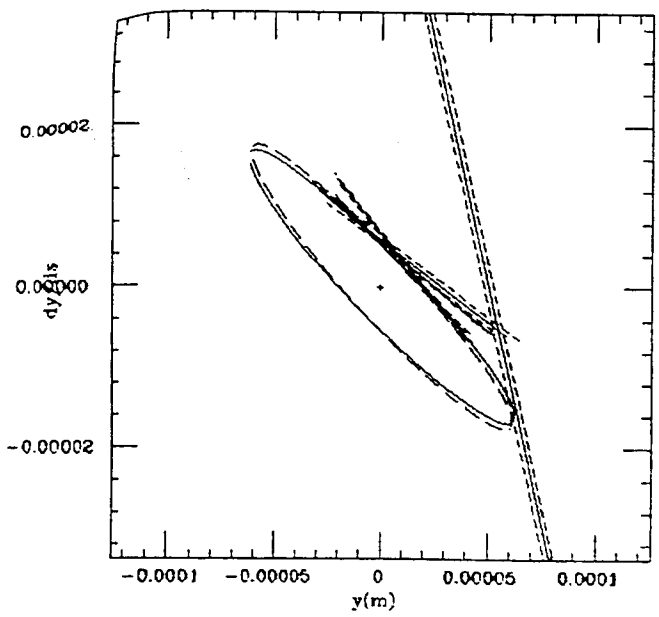

emittanceY .3365 +- .0095 (nm)
alphaY at ML5X 3.0113
betaY at ML5X 11.754 (m)
alphaY at MW0X .2686
betaY at MW0X 10.661 (m)
alphaY at MW1X -.3560
betaY at MW1X 2.8565 (m)
alphaY at MW2X .4771
betaY at MW2X 4.3252 (m)
alphaY at MW3X -3.113
betaY at MW3X 5.6650 (m)
alphaY at MW4X .8589
betaY at MW4X 22.426 (m)
BmagY 1.0182

$\epsilon_y = (33.7 \pm 1.0) \times 10^{-11}$ m.r

SET 2

$V_c = 300kV$, $\phi_{rf} = 140^\circ$
$\langle I \rangle \sim 4.5 \times 10^9$
$V_{KICK} = 29.446V$
~~V_{RF}~~ .

UNCHANGED

$\nu_x = 0.374$, $\nu_y = 0.430$
$(\Delta\nu = 0.056)$

$\sigma_y^{DR} = 28.2 \pm 0.6 \mu m$

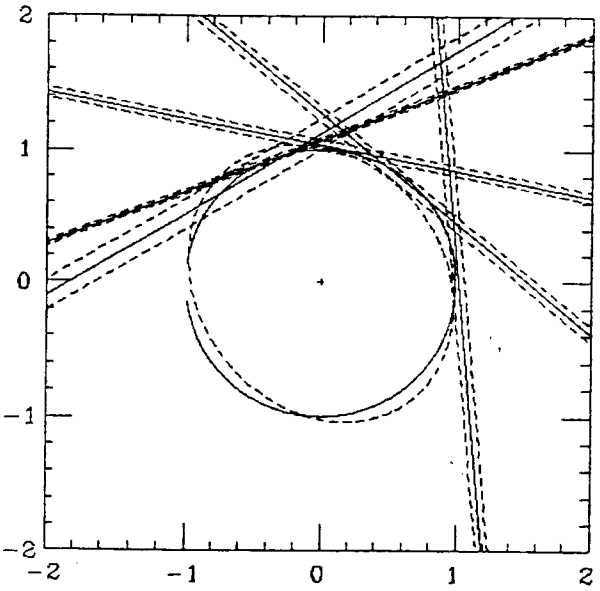

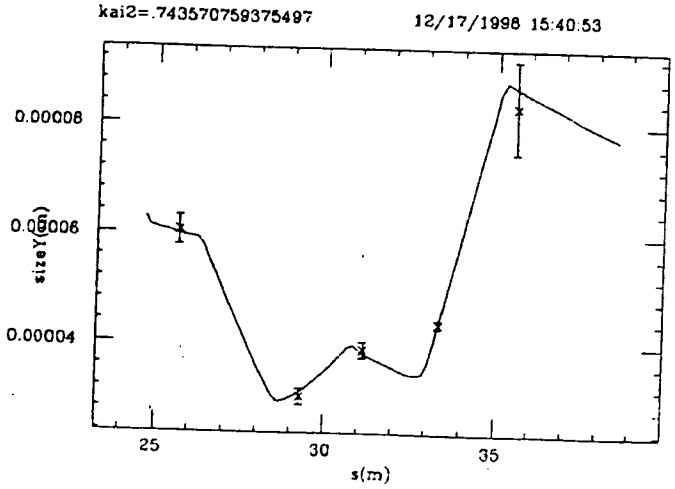

12/17/1998 15:44:56

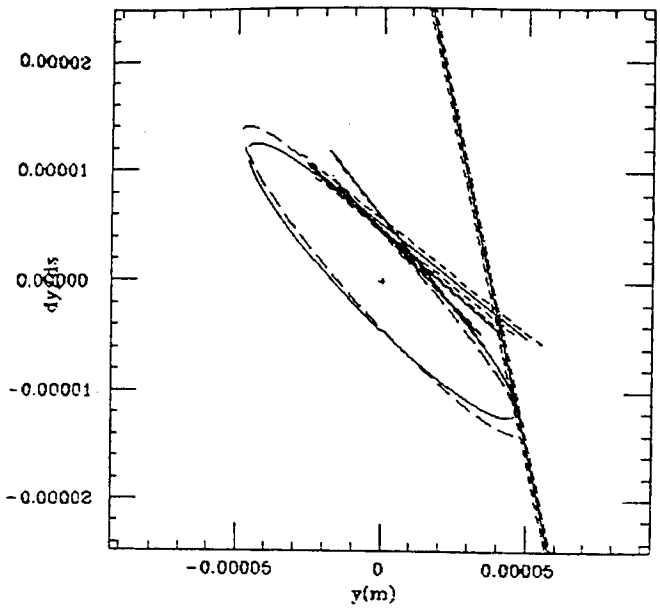

emittanceY .2096 +- .0059 (nm)
alphaY at MLSX 2.5743
betaY at MLSX 10.398 (m)
alphaY at MW0X .1315
betaY at MW0X 9.6235 (m)
alphaY at MW1X -.5083
betaY at MW1X 3.2115 (m)
alphaY at MW2X .5902
betaY at MW2X 5.0340 (m)
alphaY at MW3X -3.099
betaY at MW3X 5.9171 (m)
alphaY at MW4X 1.0044
betaY at MW4X 22.198 (m)
BmagY 1.0396

$\epsilon_y = (21.0 \pm 0.6) \times 10^{-11}$ m·r

SET 3

$V_c = 300$kV, $\phi = 140°$
$\langle I \rangle \sim 4.5 \times 10^9$
$V_{KICK} = 29.44$kV
} UNCHANGED

$\nu_x = 0.361$, $\nu_y = 0.432$
$(\Delta\nu = 0.071)$

$\sigma_y^{DR} = 24.6 \pm 0.5$ μm

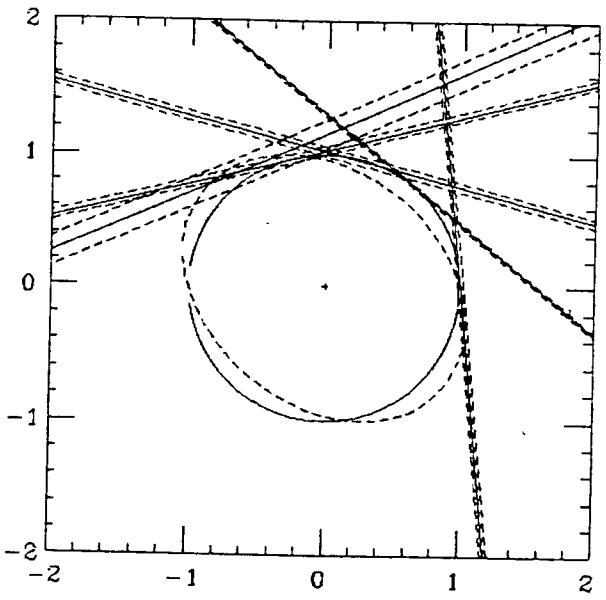

kai2=.38939352519825 12/17/1998 15:44:57

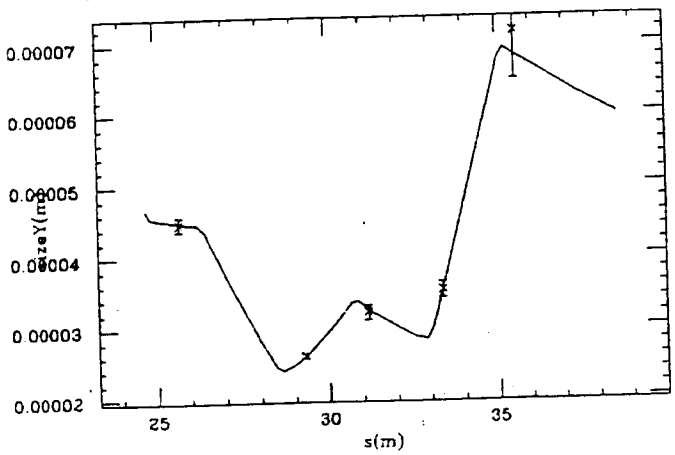

RAW DATA

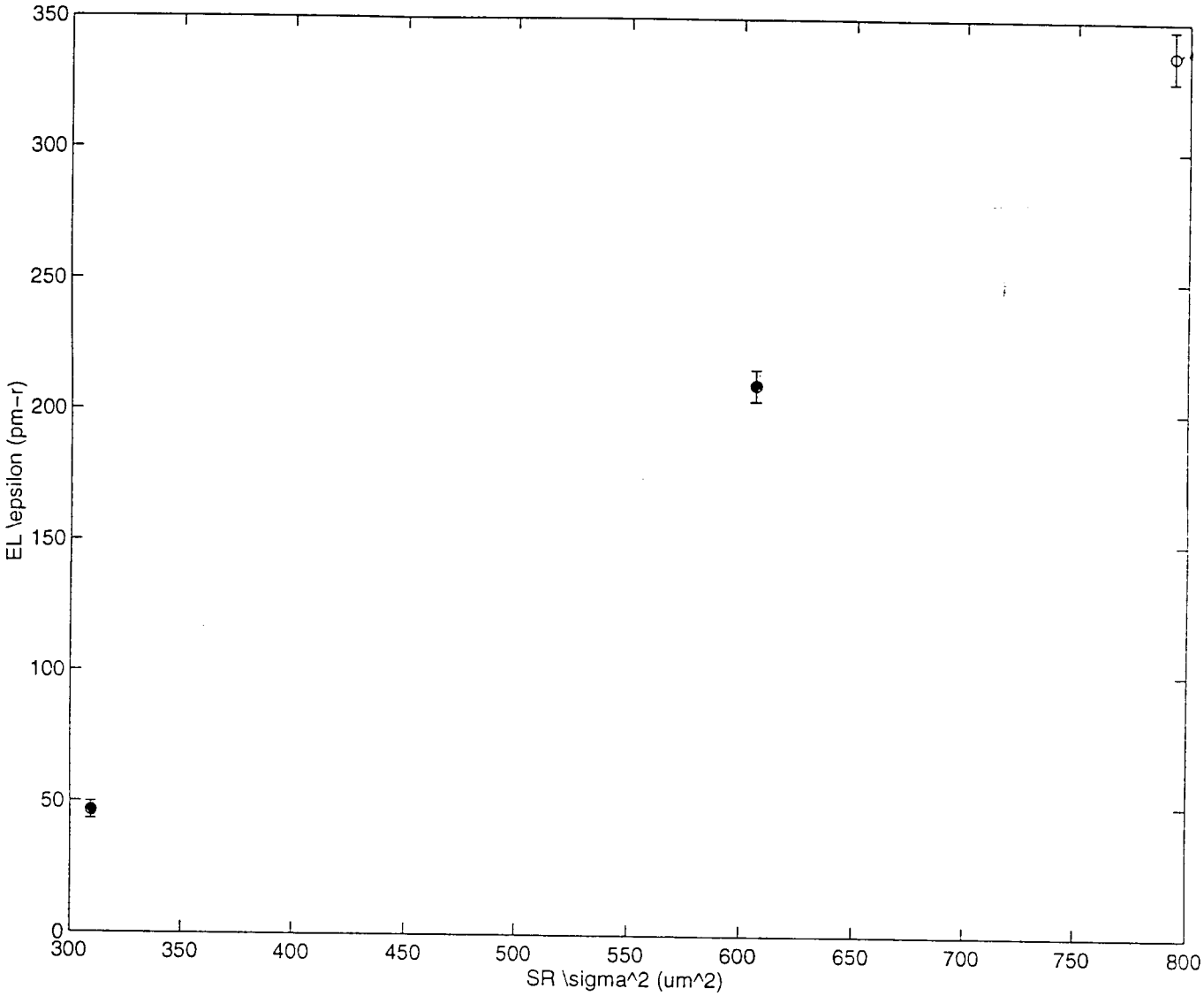

ϵ_y^{EL} = EXTRACTION LINE Y-EMITTANCE (pm·r)
(5 WIRE, ATF FIT)

σ_y^2 = DAMPING RING VERTICAL BEAM SIZE (μm^2)

1/15/99

(no Q-correction)

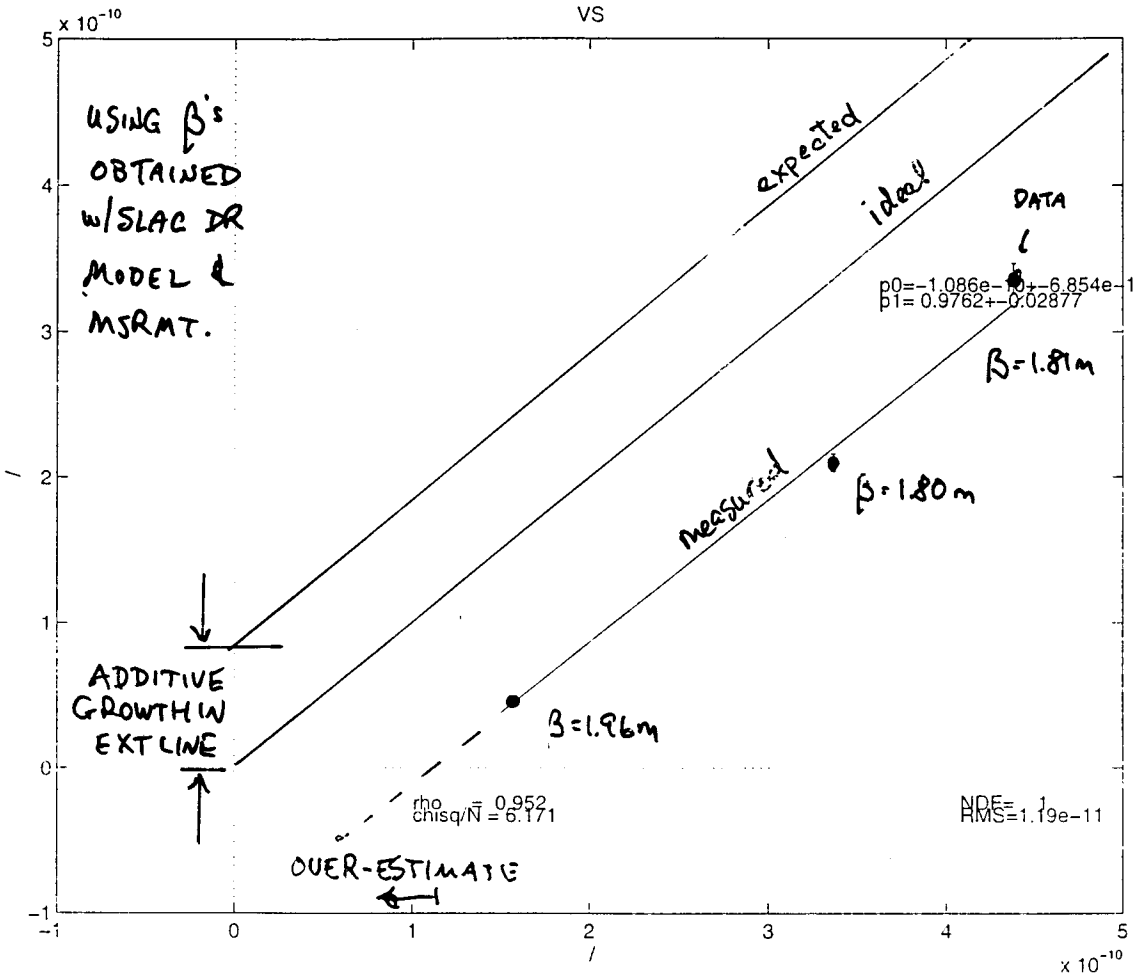

IN EITHER CASE, INTERFEROMETER SEEMS TO BE OVERESTIMATING SUBSTANTIALLY, MEASURED SPOT SIZE.

RECALL, HOWEVER THAT BY DESIGN, INTERFEROMETER GIVES UPPER BOUND.

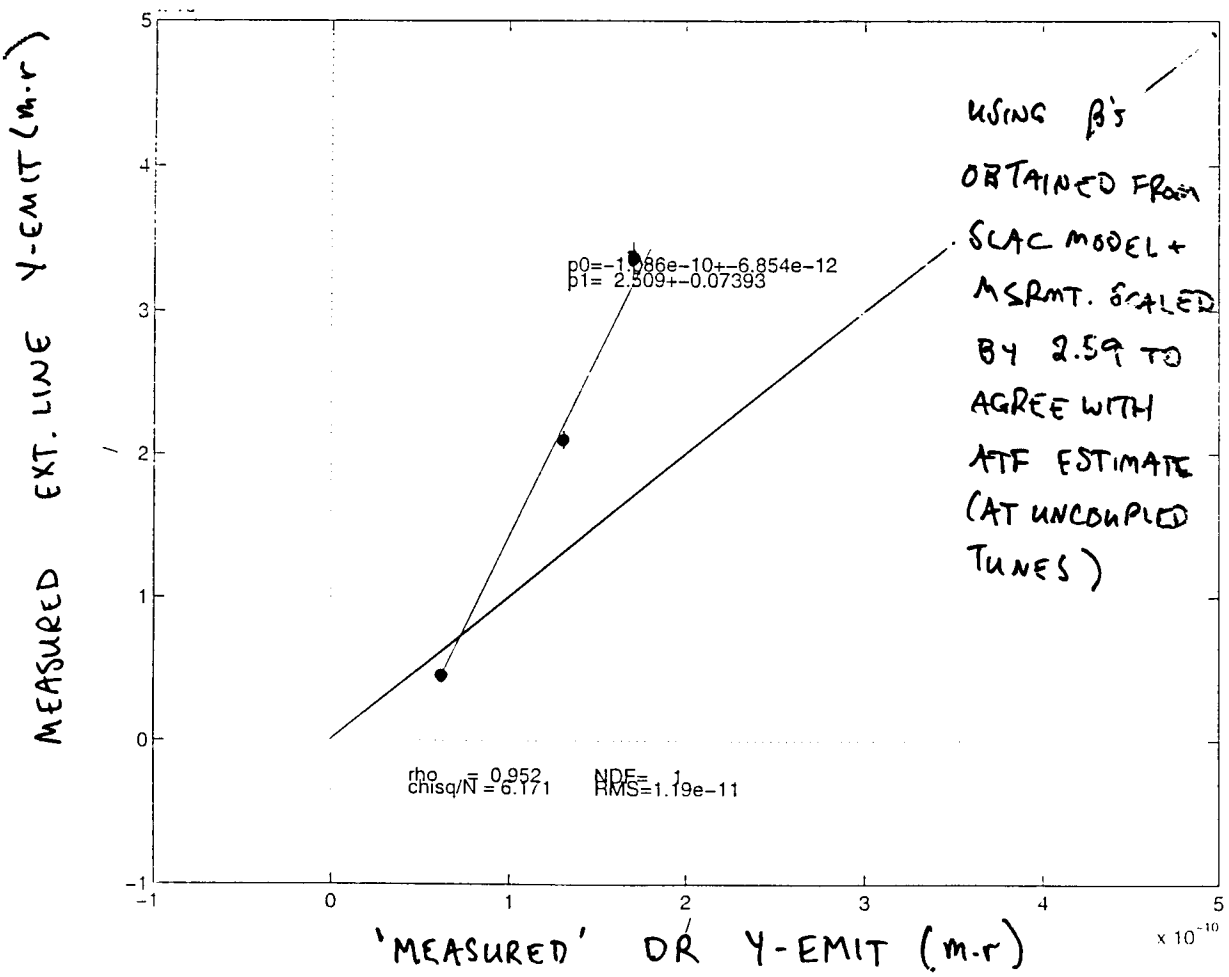

M. WOODLEY

ESTIMATION OF β. FCTN AT EMISSION POINT

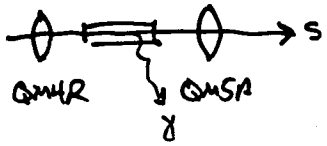

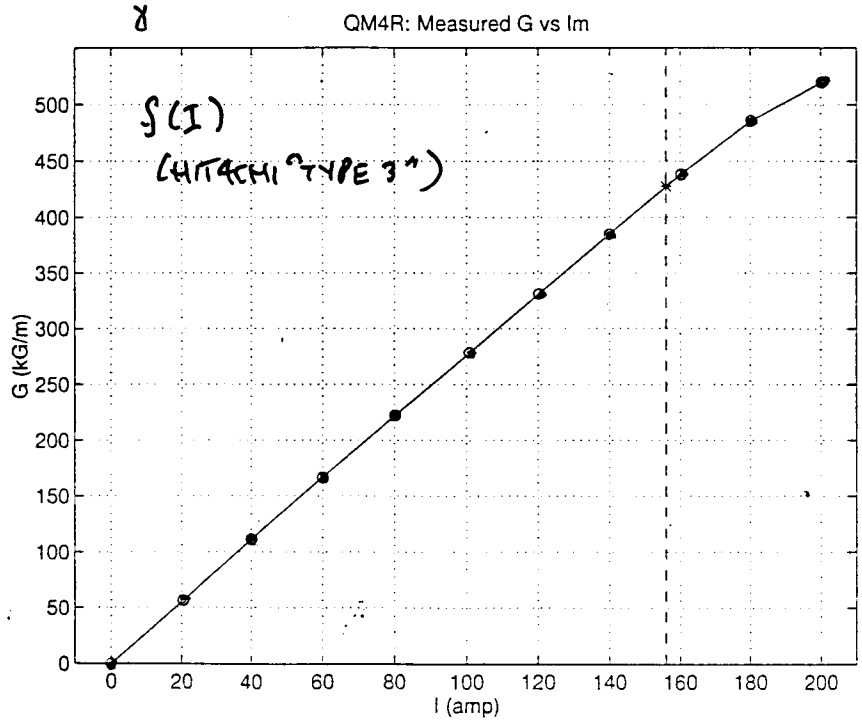

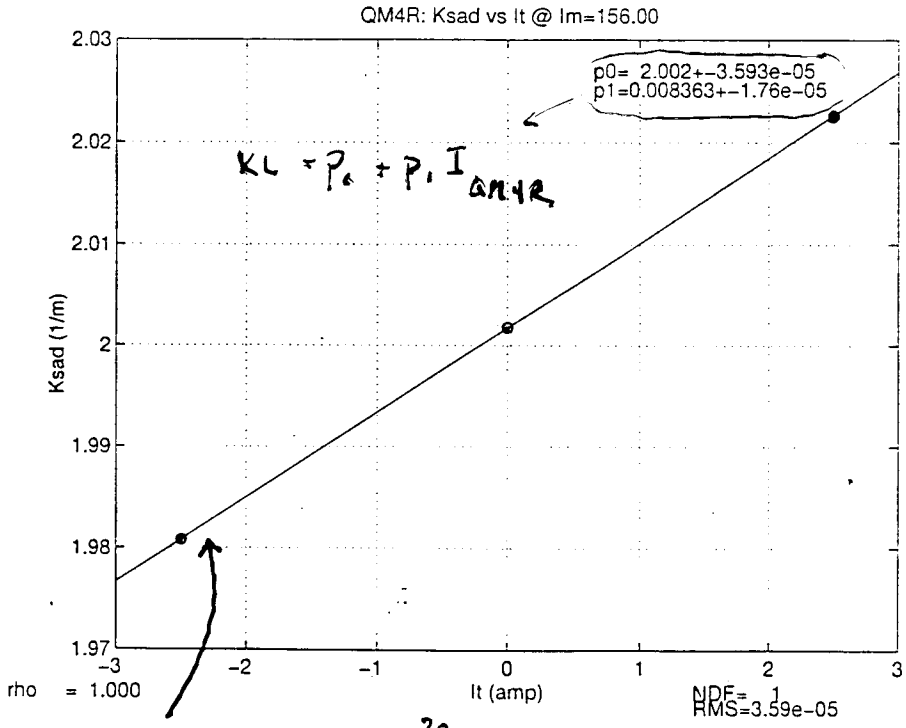

1. $K_{SAD} = f\left(I_m + \frac{N_L}{N_M} I_L\right) \cdot \frac{3 L_{eff}}{(1+F)\,100E}$ — $L_{eff} = 0.1985\,m$, $E = 1.2936\ GeV$

$\rightarrow 9.336 \times 10^{-3}$

2. AT EACH QUAD,

$$\Delta\nu = -\frac{\beta}{4\pi}(\Delta KL)$$

↑ (both quads focusing)

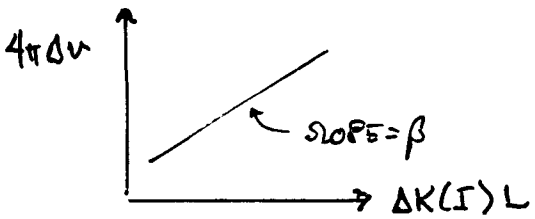

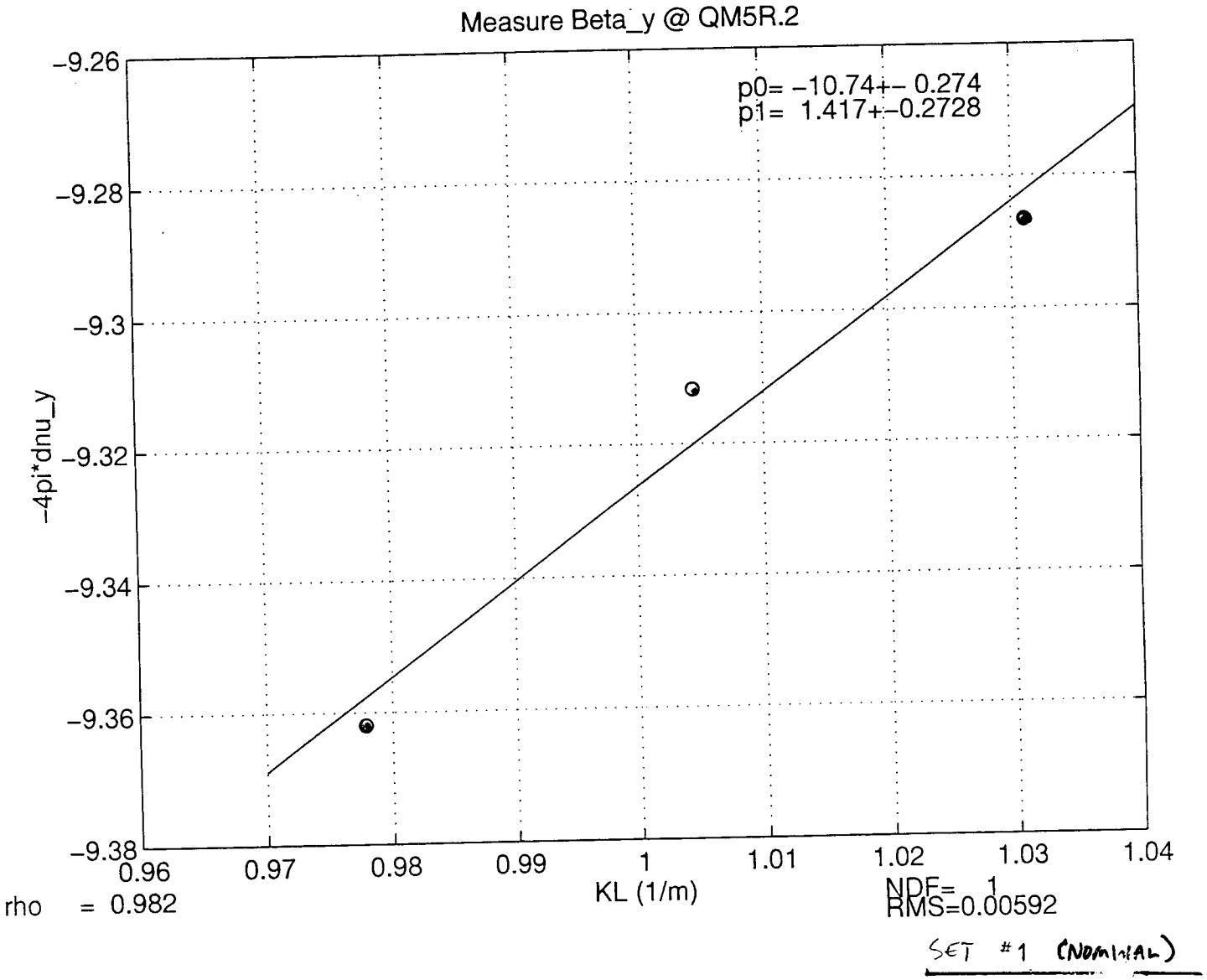

SET #1 (NOMINAL)

β_y (QM5) ≈ 1.417 m

3. AT EMISSION POINT

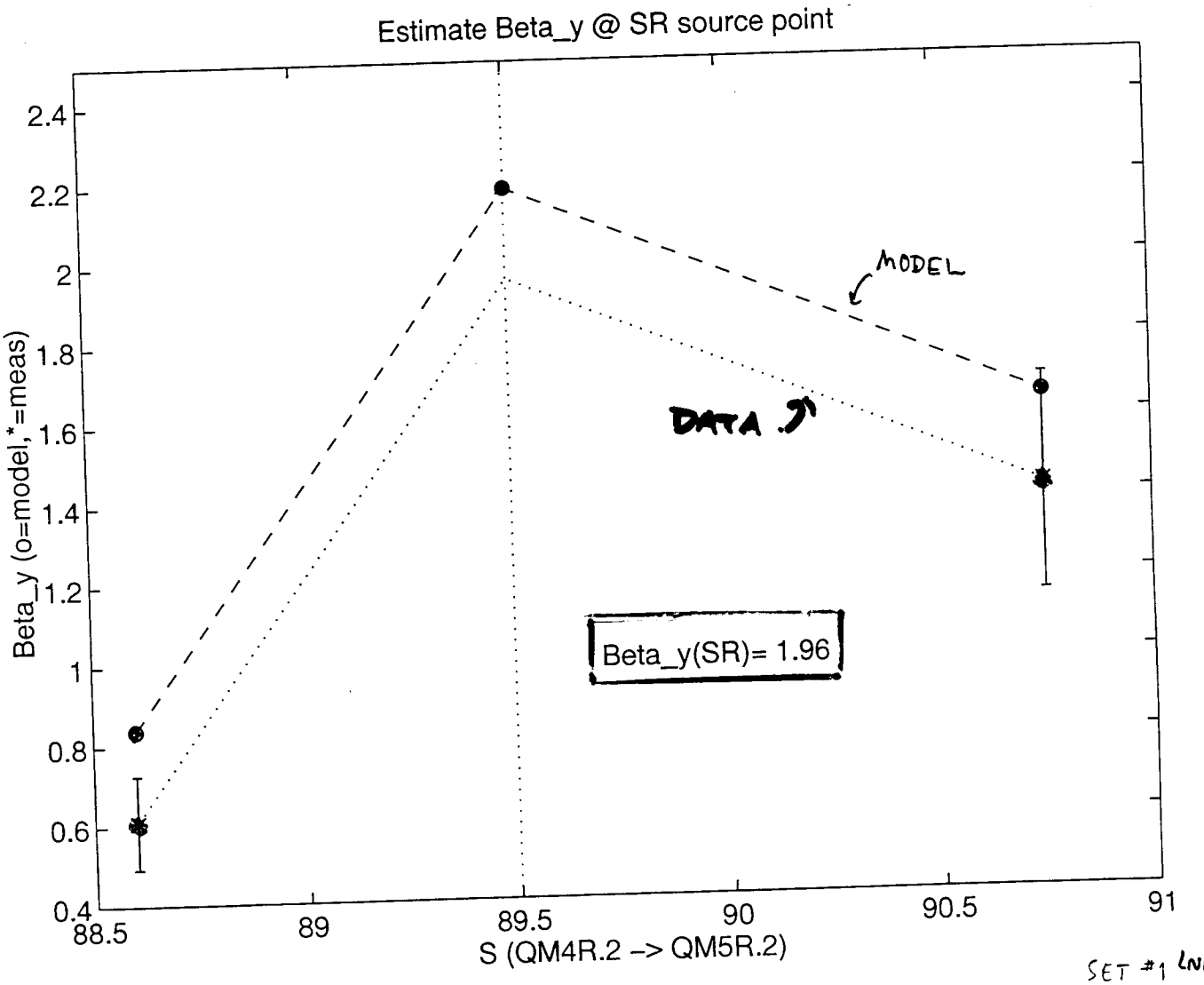

SET #1 (NOMINAL)

ESTIMATION OF η_y FCTN AT EMISSION POINT

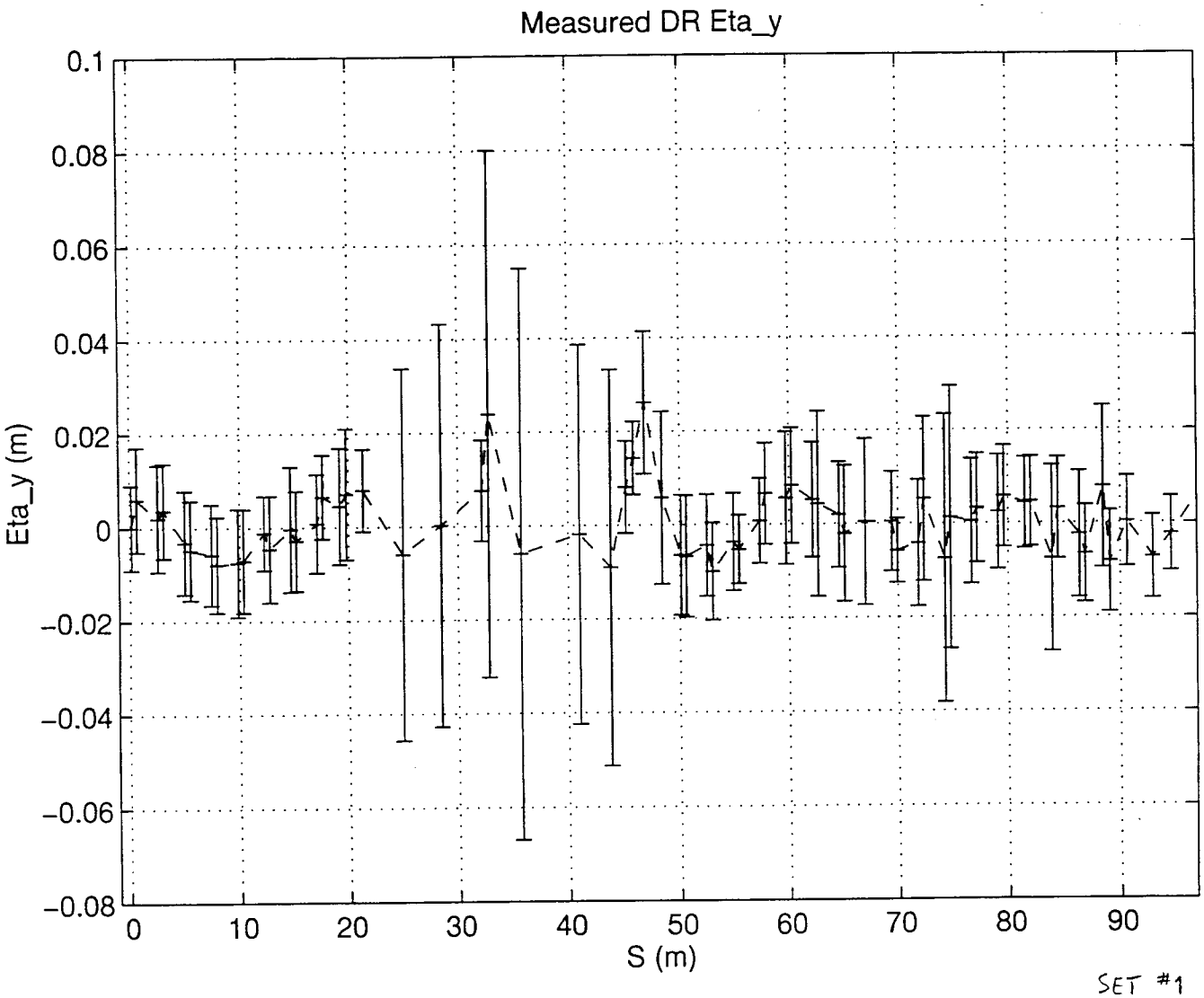

SET #1 (NOMINAL)

$\eta_y|_{BPM65} = -0.0082 \pm 0.0108\,m$

$\eta_y|_{BPM66} = +0.0003 \pm 0.0097\,m$

AVG ⇒ $\boxed{\eta_y = 4.3\,mm}$

1/24/99

COMPARISON OF VERTICAL EMITTANCE MEASUREMENTS AT THE ATF, DATA: 12/98

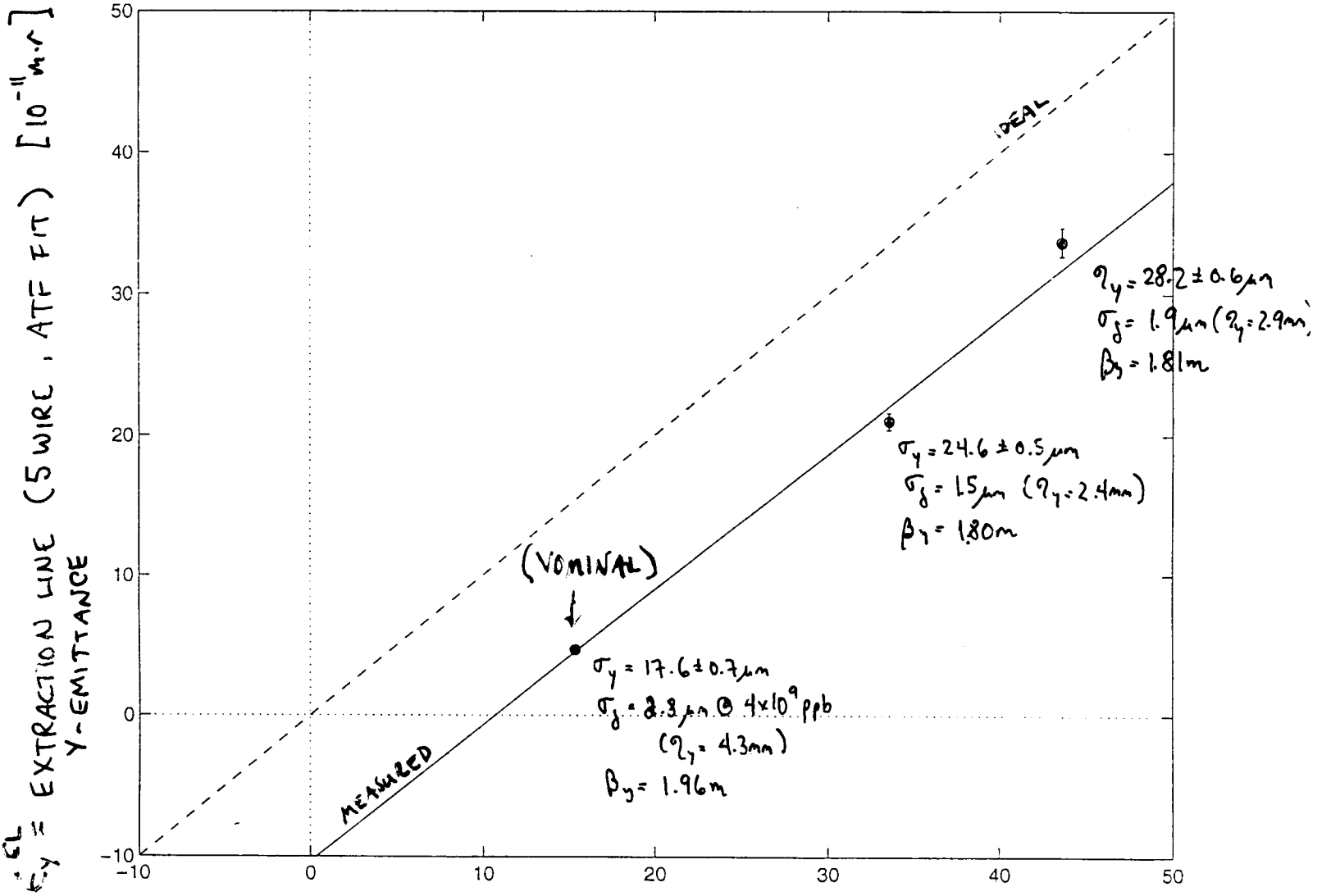

ϵ_y^{DR} = UPPER BOUND DAMPING RING EMITTANCE (INTERFEROMETER, incl'g β,η CORRECTION) $[10^{-11}\,m\cdot r]$

REPRODUCIBILITY:

12/16/98 → $\epsilon_y = (4.36 \pm 0.25)\times10^{-11}\,m\cdot r$ (ATF FIT)

$\epsilon_y = (4.11 \pm 0.16)\times10^{-11}\,m\cdot r$ (SLAC FIT)

✓ $\epsilon_{y,i} = (1.40 \pm 0.16)\times10^{-11}\,m\cdot r$ (SLAC, INTRINSIC)

12/17/98 ↳ $\epsilon_y = (4.66 \pm 0.33)\times10^{-11}\,m\cdot r$ (ATF FIT)

CONCLUSION: SR INTERFEROMETER CONSISTENTLY† OVERESTIMATES DR BEAM EMITTANCE (EXPECT 5.2 μm AT NOMINAL OPERATING POINT)

† (IN THESE DATA): WORLD RECORD $\sigma_y = 6.9\,\mu m$ ($\epsilon \sim 2.4\times10^{-11}\,m\cdot r$ w/o β,η correction) 11/98

VERTICAL EMITTANCE MEASUREMENTS AT THE ATF (NOV - DEC, 1998)

(based on WWW-posted measurement results + Dec '98 msrmts)

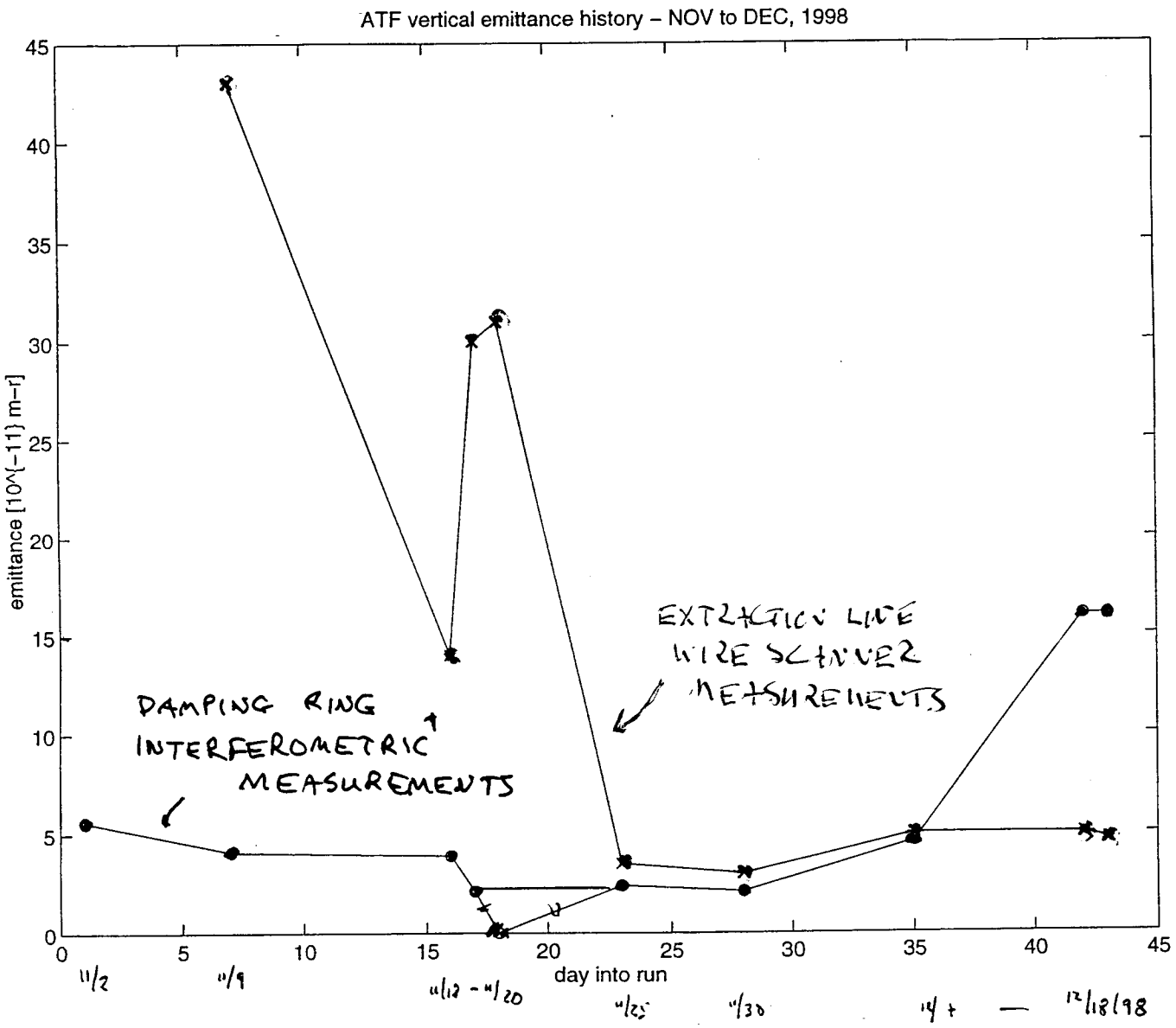

† ASSUMING $\beta_y|$ = 1.96m
emission point